INSTITUTE OF PHYSICS PUBLISHING WAVES IN RANDOM MEDIA

Waves Random Media **12** (2002) 145–173 PII: S0959-7174(02)27340-1

Monostatic and bistatic statistical shadowing functions from a one-dimensional stationary randomly rough surface according to the observation length: I. Single scattering

C Bourlier[1], **G Berginc**[2] **and J Saillard**[1]

[1] IRCCyN: UMR no 6597 CNRS, Division SETRA, Ecole Polytechnique de I'Université de Nantes, Batiment IRESTE, Rue Christian Pauc, La Chantrerie, BP 50609, 44306 Nantes Cedex 3, France
[2] DS/DFO, THALES Optronique, Rue Guynemer, BP 55, 78283 Guyancourt Cedex, France

E-mail: christophe.bourlier@polytech.univ-nantes.fr

Received 30 July 2001, in final form 31 October 2001
Published 18 December 2001
Online at stacks.iop.org/WRM/12/145

Abstract

When solving electromagnetic rough-surface scattering problems, the effect of shadowing by the surface roughness often needs to be considered, especially as the illumination angle approaches grazing incidence. This paper presents the Ricciardi–Sato, as well as the Wagner and the Smith formulations for calculating the monostatic and bistatic statistical shadowing functions from a one-dimensional rough stationary surface, which are valid for an uncorrelated Gaussian process with an infinite surface length. In this paper, these formulations are extended to include a finite surface length and any uncorrelated process. The inclusion of a finite surface length is needed to extend the single-reflection shadowing function to the more general multiple-reflection case, presented in the following companion paper. Comparisons of these shadowing functions with the exact numerical solution for the shadowing (using surfaces with Gaussian and Lorentzian autocorrelation functions for a Gaussian process) shows that the Smith formulation without correlation is a good approximation, and that including correlation only weakly improves the model. This paper also presents a method to include the shadowing effect in the electromagnetic scattering problem.

1. Introduction

Conventional theories of the scattering of electromagnetic radiation from random rough surfaces [1, 2], assume that every point of the surface contributes to the scattered wave. This assumption neglects the shadowing of the surface by itself, an effect that may be expected to be important at large angles of incidence. Under the geometrical optics approximation, Sancer [3]

showed with the Kirchhoff analysis that the scattering coefficient with shadow is obtained from the unshadowed scattering coefficient multiplied by the average shadowing function over the surface heights and slopes performed from either the Wagner [4] or Smith formulations [5, 6]. To study this assumption, Bourlier *et al* [7, 8] have investigated the statistical shadowing function, which depends on the surface heights and slopes, in the derivation of the scattering coefficient calculated from the Kirchhoff approach. They showed with a Gaussian distribution that the fact of including the statistical shadowing function modified the surface height distribution, which then becomes non-Gaussian, and carried a restriction over the surface slope distribution. This means that the expected values over the surface slopes and the surface height characteristic function have to be evaluated by including both these conditions.

Thus, an electromagnetic scattering problem with a shadowing effect from a stationary rough surface characterized by its surface height autocorrelation function and the surface slope and height joint probability density function (pdf) is similar to a problem without a shadowing effect, where the autocorrelation function is the same and the pdf is substituted by a new pdf which includes both conditions over the surface elevations and slopes. Consequently, the determination of the new pdf, equal to the unshadowed pdf multiplied by the statistical shadowing function, is the key to the problem. It is widely assumed that the statistical shadowing function is independent of the unshadowed pdf, involving moments of first and second orders with shadow being determined from the unshadowed moments multiplied by the average shadowing function.

In this paper, the statistical shadowing function from a one-dimensional rough surface is studied for monostatic (emitter and receiver locations are the same corresponding to the backscattering case) and bistatic (the emitter and receiver locations are distinct) configurations, for any uncorrelated process and for a Gaussian correlated process. Moreover, since in articles [4–8] the surface is assumed to be infinite, the effect of the observation length is introduced. In [9, 10] Bourlier *et al* have investigated this aspect of the average shadowing function for an uncorrelated Gaussian process. The inclusion of this new parameter also allows us to formulate the statistical shadowing function with multiple scattering, which will be presented in the next paper.

In section 2, the monostatic statistical shadowing function is addressed for an uncorrelated process. It depends on the surface heights and slopes, and on the parameter ν proportional to the incident beam slope divided by the surface slope rms. An additional parameter is included, which is the observation length required for the multiple-scattering problem. To select the most accurate approach, the Wagner, Smith and Ricciardi–Sato formulations are investigated for any uncorrelated process in the monostatic case and applied to a Gaussian process. As shown by Ricciardi and Sato [11, 12], the statistical shadowing function is expressed rigorously as Rice's infinite series. The Wagner approach retains only the first term of these series, whereas Smith uses the Wagner formulation by introducing a normalization function.

In section 3, to study the effect of the correlation between the surface heights and slopes, the Smith and Wagner monostatic statistical shadowing functions are compared with the numerical solutions for a Gaussian surface height and slope joint probability density function. The numerical solution, which uses any assumptions, is simulated from the algorithm developed by Brokelman and Hagfors [13]. We can note that the Ricciardi–Sato analysis with correlation is not calculated since it is not tractable analytically or numerically. The inclusion of the correlation leads to the statistical shadowing function depending on the surface height autocorrelation function. The results show that the correlation contribution is weak and the Smith formulation is close to the numerical solution.

In section 4, the uncorrelated and correlated cases are extended to a bistatic configuration for a given observation length.

The last section summarizes the obtained results, gives some prospects and discussions taking into account the shadowing effect on the electromagnetic scattering problem.

This paper develops the theoretical aspect of the shadowing effect for a given observation length, but the results are only presented for an infinite observation length. The second paper, where the statistical shadowing function with multiple scattering is investigated, presents this aspect.

2. Statistical shadowing function without correlation

Mathematical development of the shadowing function with single reflection began with the Wagner [4] and Smith [5, 6] formulations. They consider a one-dimensional surface and the correlation between the surface heights and slopes is neglected, meaning that the shadowing effect does not depend on the surface height autocorrelation function.

As shown by Ricciardi and Sato [11, 12], the statistical shadowing function is expressed rigorously as Rice's infinite series. The Wagner approach retains only the first term of these series, whereas Smith uses the Wagner formulation by introducing a normalization function. With a one-dimensional uncorrelated Gaussian process in a monostatic configuration, Bourlier *et al* [14, 15] have compared the Wagner, Smith and Ricciardi–Sato average shadowing functions with the numerical shadowing function. They proved that since the correlation is neglected the Ricciardi–Sato data have no physical meaning at grazing incidence angles, and that the Smith model is more accurate than the Wagner one.

This section extends the previous method to any uncorrelated process for a given observation length since the observation length is always assumed to be infinite for a single reflection. Unlike articles [14, 15] where the average shadowing function is presented, this section shows how the unshadowed distribution is modified by the statistical shadowing function. The observation length has to be taken into account because it is required in the multiple-scattering case.

2.1. Ricciardi–Sato, Wagner and Smith monostatic statistical shadowing functions

For an observation length L_0, the monostatic statistical shadowing function $S(\theta, F, L_0)$ is equal to the probability that the point $F(\xi_0, \gamma_0)$ on a random rough surface, of given height ξ_0 above the mean plane and with local slope $\gamma_0 = \partial\xi_0/\partial l$, is illuminated as the surface is crossed by an incident beam from incidence angle θ (figure 1) [4–6]

$$S(\mu, F, L_0) = \Upsilon(\mu - \gamma_0) \exp\left[-\int_0^{L_0} g(\mu, F, l)\,\mathrm{d}l\right], \tag{1}$$

with

$$\Upsilon(\mu - \gamma_0) = \begin{cases} 0 & \text{if} \quad \gamma_0 \geqslant \mu \\ 1 & \text{if} \quad \gamma_0 < \mu, \end{cases} \tag{1a}$$

where $g(\mu, F, l)\,\mathrm{d}l$ is the conditional probability that the ray of slope $\mu = \cot\theta$ (θ denotes the incidence angle) intersects the surface in the interval $[l; l + \mathrm{d}l]$ and with the knowledge that the ray does not cross the surface in the interval $[0; l]$. Υ is the Heaviside function, which carries a restriction on the surface slopes.

Therefore, the shadowed pdf $p_{\mathrm{Sh}}(F)$ is expressed from the unshadowed pdf $p(F)$ as

$$p_{\mathrm{Sh}}(F) = p(F) \times S(\mu, F, L_0) \qquad \text{with} \quad F \equiv F(\xi_0, \gamma_0). \tag{2}$$

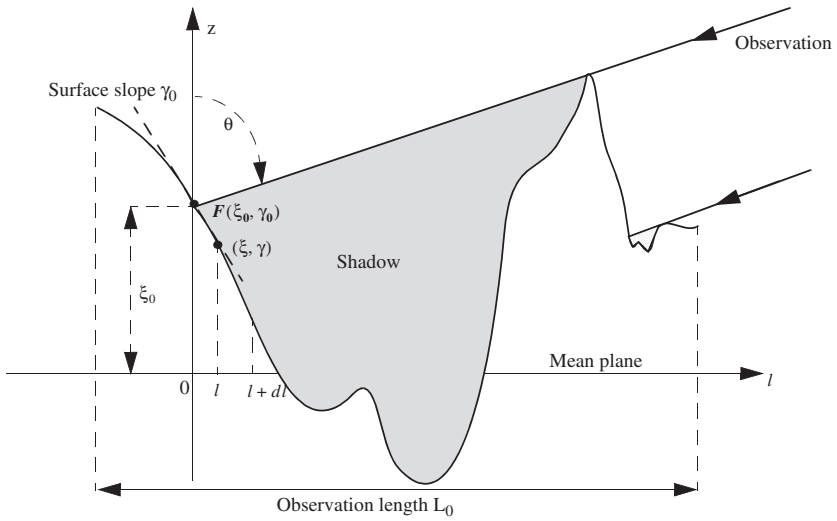

Figure 1. Statistical monostatic shadowing function.

With the Ricciardi–Sato (subscript R), Wagner (subscript W) and Smith (subscript S) approaches, $g(\mu, F, l)$ is defined as follows:

$$g_{\mathrm{R}}(\mu, F, l) = \sum_{n=0}^{\infty} (-1)^n I_n(\mu, F, l), \tag{3}$$

$$g_{\mathrm{W}}(\mu, F, l) = \int_{\mu}^{\infty} (\gamma - \mu) p(\xi, \gamma | \xi_0, \gamma_0; l)\, \mathrm{d}\gamma \qquad \xi = \xi_0 + \mu l, \tag{4}$$

$$g_{\mathrm{S}}(\mu, F, l) = g_{\mathrm{W}}(\mu, F, l) \Bigg/ \left[\int_{-\infty}^{\infty} \int_{-\infty}^{\xi_0 + \mu l} p(\xi; \gamma | \xi_0, \gamma_0; l)\, \mathrm{d}\xi\, \mathrm{d}\gamma \right], \tag{5}$$

with

$$I_0(\mu, F, l) = g_{\mathrm{W}}(\mu, F, l) \qquad \text{for} \quad n = 0$$

$$I_n(\mu, F, l) = \int_0^l \mathrm{d}l_1 \int_{l_1}^l \mathrm{d}l_2 \cdots \int_{l_{n-1}}^l W_n(\mu, F, l, l_1, \ldots, l_n)\, \mathrm{d}l_n \qquad \text{for} \quad \begin{cases} n \geqslant 1 \\ l_0 = 0, \end{cases} \tag{5a}$$

and

$$W_n(\mu, F, l, l_1, \ldots, l_n) = \int_{\mu}^{\infty} (\gamma - \mu)\, \mathrm{d}\gamma \int_{\mu}^{\infty} \mathrm{d}\gamma_1 \cdots \int_{\mu}^{\infty} \mathrm{d}\gamma_n \times \prod_{i=1}^{i=n} (\gamma_i - \mu)\, p_{2n+2}(\vec{Z}, \vec{G} | \xi_0, \gamma_0; l, l_1, \ldots, l_n), \tag{5b}$$

where $W_n(\mu, F, l, l_1, \ldots, l_n)\, \mathrm{d}l\, \mathrm{d}l_1\, \mathrm{d}l_2 \cdots \mathrm{d}l_n$ is the joint probability that the incident ray of equation $S_n = \xi_0 + \mu l_n$ ($n \geqslant 1$) crosses the surface $\xi(l_n)$, with a slope $\mu = \cot\theta$ smaller than the surface slope γ_n of abscissa l_n, in the intervals $\{[l; l + \mathrm{d}l], [l_1 l_1 + \mathrm{d}l_1], [l_2; l_2 + \mathrm{d}l_2], \ldots, [l_n; l_n + \mathrm{d}l_n]\}$, conditional on the knowledge of $F(\xi_0, \gamma_0)$. p_{2n+2} is the joint probability density of vectors $\vec{Z}^T = [\xi_0, \xi, S_1, S_2, \ldots, S_n]$ and $\vec{G}^T = [\gamma_0, \gamma, \gamma_1, \gamma_2, \ldots, \gamma_n]$ at abscissa points $\{0, l, l_1, l_2, \ldots, l_n\}$, knowing $\{\xi_0, \gamma_0\}$. The problem is slightly different from those presented in [11, 12], because the probability density p_{2n+2} is conditioned in our case by the variables $\{\xi_0, \gamma_0\}$, whereas [11, 12] only consider the term ξ_0.

We can note that the Ricciardi–Sato formulation is expressed as Rice's infinite series, and the Wagner formulation keeps only the first term of these series whereas the Smith approach uses Wagner's one and introduces a normalization function. $g_R(\mu, F, l)$ can be defined as the first passage time conditional probability density function.

2.2. *Mathematical development for any uncorrelated process*

The uncorrelated process states that

$$\begin{aligned} &p(\xi, \gamma|\xi_0, \gamma_0; l) = p(\xi_0 + \mu l)p(\gamma) \qquad \xi = \xi_0 + \mu l \\ &p_{2n+2} = p(\xi_0 + \mu l)p(\gamma)\prod_{i=1}^{i=n} p(\xi_0 + \mu l_i)p(\gamma_i). \end{aligned} \tag{6}$$

Since the cross-correlation and the correlation of the surface heights and slopes is omitted, p_{2n+2} depends only on l_i within $\xi_0 + \mu l_i$.

Substituting (6) into (3), (4) and (5*b*), we have

$$g_W(\mu, F, l) = \mu\Lambda \times p(\xi_0 + \mu l), \tag{7}$$

$$g_S(\mu, F, l) = g_W(\mu, F, l)/[P(\xi_0 + \mu l) - P(-\infty)], \tag{8}$$

$$W_n(\mu, F, l, l_1, \ldots, l_n) = g_W(\mu, F, l)\prod_{i=1}^{i=n} \mu\Lambda \times p(\xi_0 + \mu l_i), \tag{9}$$

with

$$\Lambda = \frac{1}{\mu}\int_{\mu}^{\infty} (\gamma - \mu)p(\gamma)\,\mathrm{d}\gamma, \tag{9a}$$

and P is a primitive of p defined as (A.2).

Substituting (9) into (5*a*) and (3), we show in the appendix that

$$g_R(\mu, F, l) = g_W \times \exp\{-\Lambda[P(\xi_0 + \mu l) - P(\xi_0)]\}. \tag{10}$$

Since the range of the denominator of (8) g_S is $[0; 1]$, this inverse is $[1, \infty[$, which means that $g_S \geqslant g_W$, and from (1), since $\exp(-g)$ is a decreasing function of g, we obtain $S_S(\mu, F, L_0) \leqslant S_W(\mu, F, L_0)$. Therefore, the statistical shadowing function of Smith is smaller than Wagner's whatever the assumed uncorrelated slope and height pdf. This arises from the fact that Smith introduces a normalization function in the denominator of (5).

From (10), since $\Lambda[P(\xi_0 + \mu l) - P(\xi_0)] \geqslant 0$, we obtain $g_R \leqslant g_W$, meaning that $\exp(-g_R) \geqslant \exp(-g_W)$, and for $\Lambda[P(\xi_0 + \mu l) - P(\xi_0)] \approx 0$, $g_W \approx g_R$.

In conclusion, for any uncorrelated process, the statistical shadowing functions obey the following relationship:

$$0 \leqslant S_S(\mu, F, L_0) \leqslant S_W(\mu, F, L_0) \leqslant S_R(\mu, F, L_0). \tag{11}$$

Substituting (7), (8) and (10) into (1), the integration over l leads to

$$S_{W,S,R}(\mu, F, L_0) = \Upsilon(\mu - \gamma_0) \times \Psi_{W,S,R}(\mu, \xi_0, L_0), \tag{12}$$

with

$$\Psi_W(\mu, \xi_0, L_0) = \exp\{-\Lambda[P(\xi_0 + \mu L_0) - P(\xi_0)]\}, \tag{12a}$$

$$\Psi_S(\mu, \xi_0, L_0) = \left[\frac{P(\xi_0) - P(-\infty)}{P(\xi_0 + \mu L_0) - P(-\infty)}\right]^{\Lambda}, \tag{12b}$$

$$\Psi_R = \exp(\Psi_W - 1). \tag{12c}$$

Thus, using (2), the shadowed uncorrelated pdf is then expressed as

$$p_{\mathrm{Sh}}(\mu, \xi_0, \gamma_0, L_0) = p(\gamma_0)\Upsilon(\mu - \gamma_0) \times p(\xi_0)\Psi(\mu, \xi_0, L_0). \tag{13}$$

Consequently, when the correlation is neglected, the statistical shadowing effect carries a restriction over the surface slopes γ_0 within $\Upsilon(\mu - \gamma_0)$ and modifies the surface height distribution due to the Ψ function. We can note that the restriction over the slopes is independent of the choice of formulation.

2.3. Simulations for an uncorrelated Gaussian process

A Gaussian process with zero mean and height variance ω^2 is defined as

$$p(\xi) = \frac{1}{\omega\sqrt{2\pi}} \exp\left(-\frac{\xi^2}{2\omega^2}\right) \quad \Rightarrow \quad p(\xi) = \frac{1}{2}\mathrm{erf}\left(\frac{\xi}{\omega\sqrt{2}}\right), \tag{14}$$

where erf denotes the error function and $\mathrm{erfc}(x) = 1 - \mathrm{erf}(x)$. Equations (12*a*) and (12*b*) then become for an infinite observation length L_0

$$\begin{aligned} \Psi_{\mathrm{W}}(\nu, \xi_0, \infty) &= \Psi_{\mathrm{W}}(\nu, \xi_0) = \exp\left\{-\frac{\Lambda(\nu)}{2}\mathrm{erfc}\left(\frac{\xi_0}{\omega\sqrt{2}}\right)\right\} \\ \Psi_{\mathrm{S}}(\nu, \xi_0, \infty) &= \Psi_{\mathrm{S}}(\nu, \xi_0) = \left[\frac{1}{2}\mathrm{erf}\left(\frac{\xi_0}{\omega\sqrt{2}}\right) + \frac{1}{2}\right]^{\Lambda(\nu)}. \end{aligned} \tag{15}$$

With a surface slope distribution with zero mean and slope variance σ^2, Λ (9*a*) is

$$\Lambda(\nu) = \frac{\exp(-\nu^2) - \nu\sqrt{\pi}\mathrm{erfc}(\nu)}{2\nu\sqrt{\pi}} \qquad \nu = \frac{\mu}{\sigma\sqrt{2}}. \tag{16}$$

In figure 2, the shadowed surface slope ($p_{\mathrm{Sh}}(\zeta_0) = \sigma\sqrt{2} \times p(\zeta_0)\Upsilon\ (\nu - \zeta_0)$ term of (13) plotted on the left) and height ($p_{\mathrm{Sh}}(h_0) = \omega\sqrt{2} \times p(h_0)\Psi(\nu, h_0)$ term of (13) plotted on the right) distributions are compared with the unshadowed one (crosses) according to the parameter ν and versus the normalized slope $\zeta_0 = \gamma_0/(\sigma\sqrt{2})$ and height $h_0 = \xi_0/(\omega\sqrt{2})$. We can note that $p_{\mathrm{Sh}}(\nu, \xi_0, \gamma_0)\,\mathrm{d}\xi_0\,\mathrm{d}\gamma_0 = 2\omega\sigma \times p_{\mathrm{Sh}}(\nu, h_0, \zeta_0)\,\mathrm{d}h_0\,\mathrm{d}\zeta_0$.

As seen on the left of figure 2, the area of $p_{\mathrm{Sh}}(\zeta_0)$ is inversely proportional to ν, and for $\nu = 0$ only the negative values of $p_{\mathrm{Sh}}(\zeta_0)$ are taken into account. Since $p(\zeta_0 = 2) = 0.01$, for ν larger than two the shadowing effect on the surface slopes is negligible. As depicted on the right of figure 2, for any ν, we observe that $p_{\mathrm{Sh,S}}(h_0) \leqslant p_{\mathrm{Sh,W}}(h_0) \leqslant p_{\mathrm{Sh,R}}(h_0) \leqslant p(h_0)$ (Wagner, full curve; Smith, broken curve; Ricciardi–Sato, chain curve), which is in agreement with (11). Moreover, the shadowing effect on the surface height distribution increases when ν decreases due to the fact that (16) Λ increases. For small values of $x = \Lambda \times \mathrm{erfc}(h_0)/2$, we have $\Psi_{\mathrm{R}} = \exp(\mathrm{e}^{-x} - 1) \approx \exp(-x) = \Psi_{\mathrm{W}}$, which explains why the deviation between the Wagner and Ricciardi–Sato results is close to zero for $h_0 > 1(\mathrm{erfc}(1)/2 = 0.0786)$ and $\Lambda \ll 1$.

In conclusion, if $\nu \geqslant 2$, then the shadowing effect on the surface heights and slopes can be omitted and $p_{\mathrm{Sh}}(\mu, \xi_0, \gamma_0) \approx p(\xi_0, \gamma_0)$. Physically, with a surface slope rms σ equal to 0.4, figure 2 represents the distribution of the surface heights and slopes for incidence angles $\theta = \mathrm{arccot}(\nu\sigma\sqrt{2}) = \{60.5^\circ, 74.2^\circ, 86.8^\circ\}$.

The statistical shadowing function integrated over the surface heights and slope is defined as

$$\begin{aligned} S(\nu, L_0) &= \int_{-\infty}^{\infty}\int_{-\infty}^{\infty} p_{\mathrm{Sh}}(\nu, \xi_0, \gamma_0, L_0)\,\mathrm{d}\xi_0\,\mathrm{d}\gamma_0 \\ &= \int_{-\infty}^{\infty}\int_{-\infty}^{\infty} p(\xi_0, \gamma_0) S(\nu, \xi_0, \gamma_0, L_0)\,\mathrm{d}\xi_0\,\mathrm{d}\gamma_0. \end{aligned} \tag{17}$$

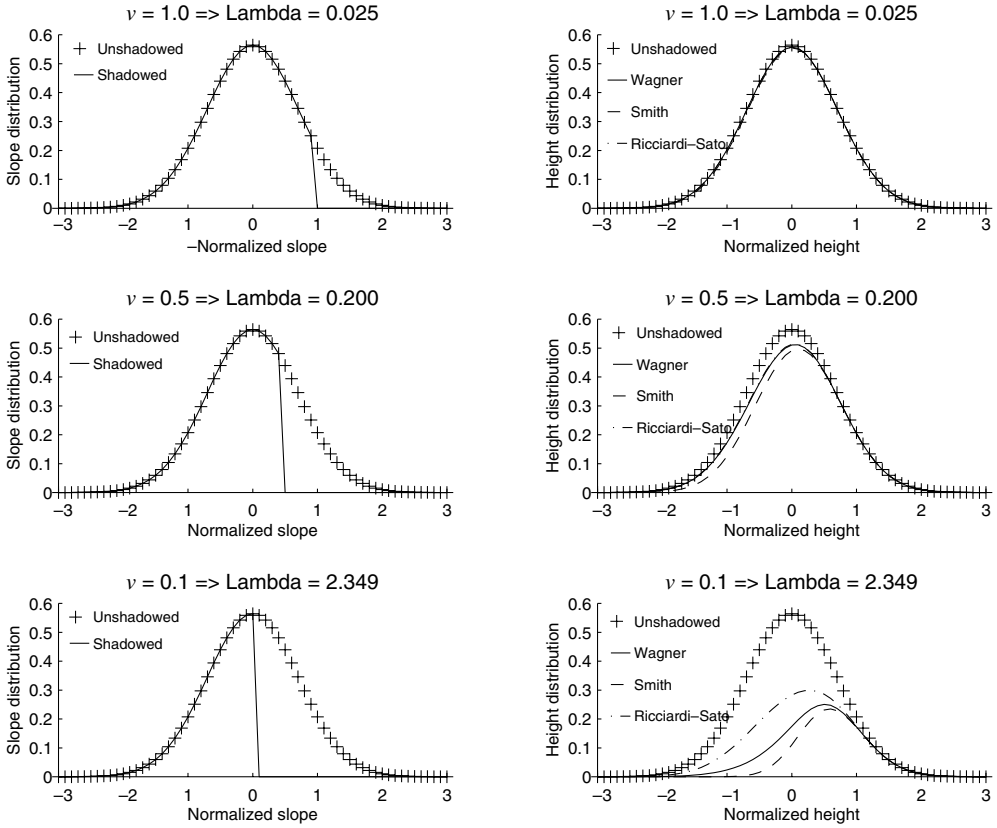

Figure 2. Comparison of the shadowed and unshadowed monostatic distributions of the surface slopes (left) and heights (right) according to the parameter ν and versus the normalized surface slopes $\zeta_0 = \gamma_0/(\sigma\sqrt{2})$ and heights $h_0 = \xi_0/(\omega\sqrt{2})$.

This corresponds to the average shadowing function. Using (12*a*)–(12*c*) (the Wagner, Smith and Ricciardi–Sato statistical shadowing functions for any uncorrelated distribution), the integration over $\{\xi_0, \gamma_0\}$ yields with an infinite observation length (see appendices 1 and 2 of [14])

$$\begin{aligned} S_{\mathrm{W}}(\nu) &= \Lambda_1 \times [1 - \exp(-\Lambda)]/\Lambda \\ S_{\mathrm{S}}(\nu) &= \Lambda_1/(1 + \Lambda) \\ S_{\mathrm{R}}(\nu) &= \Lambda_1[E_1(-\mathrm{e}^{-\Lambda}) - E_1(-1)]/\Lambda\mathrm{e}^1), \end{aligned} \tag{18}$$

where E_1 is the integral exponential function defined as

$$E_1(x) = \int_1^{\infty} \frac{\mathrm{e}^{-xt}}{t}\,\mathrm{d}t, \tag{18a}$$

and Λ_1 given by

$$\Lambda_1(\nu) = \sigma\sqrt{2}\int_{-\infty}^{\nu} p(\sigma\sqrt{2}\gamma_0)\,\mathrm{d}\gamma_0. \tag{19}$$

We can note that the $S_{\mathrm{R}}(\nu)$ expression is only valid for a Gaussian surface height distribution.

In figure 3 the one-dimensional average monostatic shadowing functions $S_{\mathrm{W,S,R}}(\nu)$ for an uncorrelated Gaussian process ($\Lambda_1(\nu) = [1 + \mathrm{erf}(\nu)]/2$ and $\Lambda(\nu)$ given by (16)) are plotted

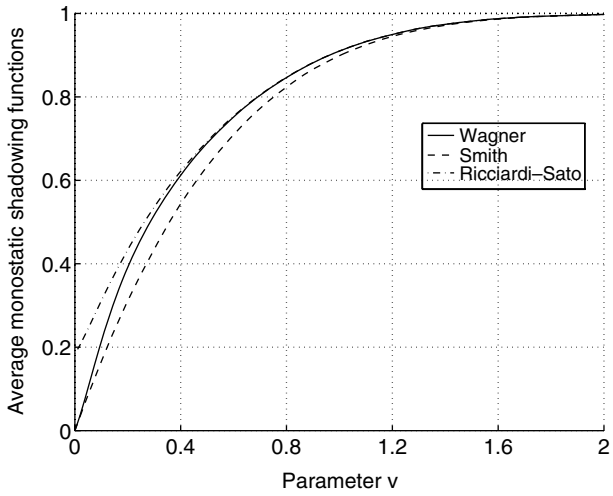

Figure 3. Comparison of Wagner (full curve), Smith (broken curve) and Ricciardi–Sato (chain curve) one-dimensional average monostatic shadowing functions $S_{\mathrm{W,S,R}}$ for an uncorrelated Gaussian process.

versus ν. We observe that Smith's results (broken curve) are smaller than Wagner's (full curve), meaning that (11) is also verified for the average shadowing function. The Wagner and Ricciardi–Sato (chain curve) results are equal for $\nu \geqslant 0.6$, whereas they differ for smaller values, corresponding to incidence angles close to 90°. Indeed,

$$S_{\mathrm{R}}(0) = \mathrm{e}^{-1}/2 = 0.184 \qquad \text{and} \qquad S_{\mathrm{W}}(0) = 0. \tag{20}$$

Physically the shadowing function is equal to zero at a grazing angle of 90°. Thus, when the correlation is not included, the Sato–Ricciardi results do not give satisfying results at grazing angles, whereas the Wagner results are correct but overestimate the shadowing function (see section 3.2). As shown previously, when ν is larger than 2, the average shadowing function is equal to unity, meaning that the shadowing effect is not required.

Since the correlation is not introduced, the statistical shadowing function does not depend on the surface height autocorrelation. To study this dependence, the next section presents the Smith and Wagner formulations for a Gaussian surface height and slope joint process. The complexity of (3) does not allow us to analytically and numerically compute the function g_{R}.

3. Statistical shadowing function with correlation

In this section, the correlation between the surface heights and slopes is investigated for a Gaussian process for any surface height autocorrelation function. Bourlier *et al* [14, 15] have studied this case for the average monostatic shadowing function for an infinite observation length. Therefore, their approach is summarized to explain the method and is applied in the derivation of the statistical shadowing function with a given observation length. In the multiple-scattering problem, the observation length is required. The simulations present the statistical shadowing function with the derivations of marginal probabilities and cumulative functions of the surface heights and slopes.

3.1. Formulation with correlation

For a Gaussian surface height $\{\xi, \xi_0\}$ and slope $\{\gamma, \gamma_0\}$ joint process, $p(\xi, \gamma|\xi_0, \gamma_0; l)$, is expressed as (appendix 3 of [14])

$$p(\xi, \gamma|\xi_0, \gamma_0; l) = \frac{\sigma\omega}{2\pi\sqrt{|[C]|}} \times \exp\left[-\frac{C_{i11}(\xi_0^2 + \xi^2) + C_{i33}(\gamma_0^2 + \gamma^2)}{2|[C]|} + \frac{\xi_0^2}{2\omega^2} + \frac{\gamma_0^2}{2\sigma^2} - \frac{2C_{i12}\xi_0\xi + 2C_{i34}\gamma_0\gamma + 2C_{i13}(\xi_0\gamma_0 - \xi\gamma) + 2C_{i14}(\xi_0\gamma - \xi\gamma_0)}{2|[C]|} \right], \tag{21}$$

with

$$\begin{aligned} C_{i11} &= \omega^2(\sigma^4 - R_2^2) - R_1^2\sigma^2 & C_{i14} &= R_1(R_1^2 - R_0R_2 - \omega^2\sigma^2) \\ C_{i12} &= R_0(R_2^2 - \sigma^4) - R_1^2R_2 & C_{i33} &= \sigma^2(\omega^4 - R_0^2) - R_1^2\omega^2 \\ C_{i13} &= -R_1(R_0\sigma^2 + \omega^2R_2) & C_{i34} &= R_2(\omega^4 - R_0^2) + R_1^2R_0 \\ |[C]| &= (C_{i33}^2 - C_{i34}^2)/(\omega^4 - R_0^2) \end{aligned} \tag{21a}$$

where $R_0(l)$ is the autocorrelation function, assumed to be even and derivable at the origin, and $\{R_1(l), R_2(l)\}$ are its first and second derivatives. The surface height variance ω^2 is equal to $R_0(0)$ and the surface slope variance σ^2 is $-R_2(0)$. $|[C]|$ is the determinant of the covariance matrix $[C]$. The first index i in C_{ij} denotes the elements of the inverse matrix $[C]$ defined as

$$[C] = \begin{bmatrix} \omega^2 & R_0(l) & 0 & R_1(l) \\ R_0(l) & \omega^2 & -R_1(l) & 0 \\ 0 & -R_1(l) & \sigma^2 & -R_2(l) \\ R_1(l) & 0 & -R_2(l) & \sigma^2 \end{bmatrix}. \tag{22}$$

If the correlation is neglected, then $[C]$ is diagonal, and (21) becomes (6).

Using the equation

$$\int_\mu^\infty (\gamma - \mu)\exp(-A\gamma^2 - 2B\gamma - D)\,\mathrm{d}\gamma = \frac{\exp[-D - \mu(\mu A + 2B)]}{2A}[1 - \exp(\kappa^2)\kappa\sqrt{\pi}\operatorname{erfc}(\kappa)], \tag{23}$$

with $\kappa = (B + \mu A)/\sqrt{A}$, the integration over γ of (4) yields

$$g_{\mathrm{W}}(\mu, F, l) = \frac{\sigma\omega\exp[-D - \mu(\mu A + 2B)]}{4\pi A\sqrt{|[C]|}}[1 - \exp(\kappa^2)\kappa\sqrt{\pi}\operatorname{erfc}(\kappa)], \tag{24}$$

where

$$\begin{aligned} A &= \frac{C_{i33}}{2|[C]|} \qquad B = \frac{\xi_0 C_{i14} - \xi C_{i13} + \gamma_0 C_{i34}}{2|[C]|} \qquad \xi = \xi_0 + \mu l \\ D &= \frac{(\xi_0^2 + \xi^2)C_{i11} + 2\xi_0\xi C_{i12} + 2\gamma_0(\xi_0 C_{i13} - \xi C_{i14}) + \gamma_0^2 C_{i33}}{2|[C]|} - \frac{\xi_0^2}{2\omega^2} - \frac{\gamma_0^2}{2\sigma^2}. \end{aligned} \tag{24a}$$

With the Smith formulation (5), applying (23) and the relationship

$$\int_{-\infty}^{\xi'} \exp(-A_1\xi^2 - 2B_1\xi - D_1)\,\mathrm{d}\xi = \frac{1}{2}\sqrt{\frac{\pi}{A_1}}\exp\left(\frac{B_1^2}{A_1} - D_1\right)\left[\operatorname{erf}\left(\frac{A_1\xi' + B_1}{\sqrt{A_1}}\right) + 1\right], \tag{25}$$

the integrations over $\{\gamma, \xi\}$ give

$$g_{\mathrm{S}}(\mu, F, l) = \frac{1}{\pi}\sqrt{\frac{A_1}{A}}\frac{\exp[-D - \mu(\mu A + 2B) - \frac{\xi_0^2}{2\omega^2} - \frac{\gamma_0^2}{2\sigma^2}][1 - \exp(\kappa^2)\kappa\sqrt{\pi}\operatorname{erfc}(\kappa)]}{\exp(\frac{B_1^2}{A_1} - D_1)\{\operatorname{erf}(\frac{A_1\xi + B_1}{\sqrt{A_1}}) + 1\}}, \tag{26}$$

where

$$\begin{aligned}
&A_1 = (C_{i11}C_{i33} - C_{i13}^2)E_1 \qquad E_1 = 1/(2C_{i33}|[C]|)\\
&B_1 = [\xi_0(C_{i12}C_{i33} + C_{i14}C_{i13}) + \gamma_0(C_{i13}C_{i34} - C_{i14}C_{i33})]E_1\\
&D_1 = [\xi_0^2(C_{i11}C_{i33} - C_{i14}^2) + \gamma_0^2(C_{i33}^2 - C_{i34}^2) + 2\xi_0\gamma_0(C_{i13}C_{i33} - C_{i14}C_{i34})]E_1.
\end{aligned} \tag{26a}$$

To express the statistical shadowing function over ν, we set

$$R_0 = \omega^2 f_0 \qquad R_1 = -\sigma\,\omega f_1 \qquad R_2 = -\sigma^2 f_2. \tag{27}$$

Substituting (27) into (21a), we obtain

$$\begin{aligned}
&\frac{C_{i11}}{2|[C]|} = \frac{1}{2\omega^2}\frac{f_{11}}{f_M} \qquad \frac{C_{i33}}{2|[C]|} = \frac{1}{2\sigma^2}\frac{f_{33}}{f_M} \qquad \frac{C_{i13}}{2|[C]|} = \frac{1}{2\sigma\omega}\frac{f_{13}}{f_M}\\
&\frac{C_{i12}}{2|[C]|} = \frac{1}{2\omega^2}\frac{f_{12}}{f_M} \qquad \frac{C_{i34}}{2|[C]|} = \frac{1}{2\sigma^2}\frac{f_{34}}{f_M} \qquad \frac{C_{i14}}{2|[C]|} = \frac{1}{2\sigma\omega}\frac{f_{14}}{f_M}\\
&|[C]| = f_M(\omega\sigma)^4,
\end{aligned} \tag{28}$$

with

$$\begin{aligned}
&f_{11} = 1 - f_2^2 - f_1^2 \qquad f_{33} = 1 - f_0^2 - f_1^2 \qquad f_{13} = f_1(f_0 - f_2)\\
&f_{12} = f_0 f_2^2 + f_1^2 f_2 - f_0 \qquad f_{34} = f_0^2 f_2 + f_1^2 f_0 - f_2\\
&f_{14} = f_1(1 - f_1^2 - f_0 f_2) \qquad f_M = (f_{33}^2 - f_{34}^2)/(1 - f_0^2).
\end{aligned} \tag{28a}$$

Using the variable transformations

$$h_0 = \xi_0/(\omega\sqrt{2}) \qquad \zeta_0 = \gamma_0/(\sigma\sqrt{2}) \qquad y = l/L_{\mathrm{c}}, \tag{29}$$

where L_{c} denotes the surface correlation length, $g_{\mathrm{W,S}}(\nu, h_0, \zeta_0, y)L_{\mathrm{c}}$ is expressed in table 1. We can note that f_{ij} depends on y.

When the correlation is neglected we have $R_{0,1,2} = 0$, which involves $f_{0,1,2} = 0$ and from (28a) $f_{ij} = \delta_{ij}$ (Kronecker symbol) with $\delta_{ij} = 1$ if $i = j$, else 0. From table 1, we obtain

$$\begin{aligned}
&g_{\mathrm{W}}(\nu, h_0, \zeta_0, y)L_{\mathrm{c}} = \eta\nu\Lambda\exp[-(h_0 + \eta\nu y)^2]/\sqrt{\pi}\\
&g_{\mathrm{S}}(\nu, h_0, \zeta_0, y)L_{\mathrm{c}} = g_{\mathrm{W}} \times 2/[1 + \mathrm{erf}\,(h_0 + \eta\nu y)].
\end{aligned} \tag{30}$$

Therefore, the above equations are similar to (7) and (8) (uncorrelated case with a Gaussian process $p(\xi) = \exp(-\xi^2)/(\omega\sqrt{2\pi})$) with $\eta\nu = \mu L_{\mathrm{c}}/(\omega\sqrt{2})$ and $y = l/L_{\mathrm{c}}$.

In figure 4 the functions f_{ij} are plotted versus y for Gaussian and Lorentzian surface height autocorrelation functions (table 2). We observe that the functions $\{f_{12}, f_{34}, f_{13}, f_{14}\}$ $(i \neq j)$ become equal to zero when $y \geqslant y_{t\mathrm{G}} = 3$ and $y \geqslant y_{t\mathrm{L}} = 4$ in the Gaussian (broken curve) and Lorentzian (chain curve) cases respectively, whereas $\{f_{11}, f_{33}\}$ $(i = j)$ become independent of y and tend to unity. In the uncorrelated case represented in the full curve, $\{f_{ij}\}$ is equal to either zero or one. Therefore, in the range $[y_i; \infty[$, the correlation can be neglected and (30) is valid, whereas for $[0; y_t]$ $g_{\mathrm{W,S}}(\nu, h_0, \zeta_0, y)$ has to be computed from table 1.

Thanks to this property, we can write with $y_0 = L_0/L_{\mathrm{c}} > y_t$ (normalized observation length) that

$$L_{\mathrm{c}}\int_0^{y_0} g_{\mathrm{W,S}}(\nu, h_0, \zeta_0, y)\,\mathrm{d}y = L_{\mathrm{c}}\int_0^{y_t} g_{\mathrm{W,S}}(\nu, h_0, \zeta_0, y)\,\mathrm{d}y + G_{\mathrm{W,S}}(\nu, h_0, y_t, y_0), \tag{31}$$

with

$$G_{\mathrm{W,S}}(\nu, h_0, y_t, y_0) = L_{\mathrm{c}}\int_{y_t}^{y_0 \geqslant y_t} g_{\mathrm{W,S}}(\nu, h_0, y)\,\mathrm{d}y, \tag{31a}$$

Table 1. Wagner and Smith monostatic statistical shadowing functions for a correlated Gaussian process with the variable transformations $h_0 = \xi_0/(\omega\sqrt{2})$, $\zeta_0 = \gamma_0/(\sigma\sqrt{2})$, and $y = l/L_c$.

Statistical shadowing function	$S(\nu, h_0, \zeta_0, y_0) = \Upsilon(\nu - \zeta_0)\exp\left[-L_c\int_0^{y_0=L_0/L_c} g(\nu, h_0, \zeta_0, y)\,dy\right]$
Wagner function $L_c g(\nu, h_0, \zeta_0, y)$	$\frac{\eta\sqrt{f_M}}{2\pi f_{33}}\exp[-D - \nu(\nu A + 2B)][1 - \exp(\kappa^2)\kappa\sqrt{\pi}\operatorname{erfc}(\kappa)]$ $\kappa = (B + \nu A)/\sqrt{A} \qquad \eta = \sigma L_c/\omega = \text{constant}$ $\begin{cases} D = \dfrac{(h_0^2 + h^2)f_{11} + 2h_0 h f_{12} + 2\zeta_0(h_0 f_{13} - h f_{14}) + \zeta_0^2 f_{33}}{f_M} - h_0^2 - \zeta_0^2 \\ \nu(\nu A + 2B) = \dfrac{\nu^2 f_{33} + 2\nu(f_{34}\zeta_0 + h_0 f_{14} - h f_{13})}{f_M} \qquad h = h_0 + y\nu\eta \\ \kappa = \dfrac{h_0 f_{14} - h f_{13} + \zeta_0 f_{34} + \nu f_{33}}{\sqrt{f_{33} f_M}} \end{cases}$
Wagner function $G_W(\nu, h_0, y_t, y_0)$	$\frac{\Lambda(\nu)}{2}[\operatorname{erf}(h_0 + y_0\nu\eta) - \operatorname{erf}(h_0 + y_t\nu\eta)]$
Smith function $L_c g(\nu, h_0, \zeta_0, y)$	$\frac{\eta}{\pi}\dfrac{\sqrt{f_{11}f_{33} - f_{13}^2}}{f_{33}}\dfrac{\exp[-D - \nu(\nu A + 2B) - h_0^2 - \zeta_0^2][1 - \exp(\kappa^2)\kappa\sqrt{\pi}\operatorname{erfc}(\kappa)]}{e^{\frac{B_1^2}{A_1} - D_1}\left[1 + \operatorname{erf}\left(\sqrt{A_1}h + \frac{B_1}{\sqrt{A_1}}\right)\right]}$ $\begin{cases} D_1 = h_0^2\dfrac{f_{11}f_{33} - f_{14}^2}{f_{33}f_M} + \zeta_0^2\dfrac{f_{33}^2 - f_{34}^2}{f_{33}f_M} + 2h_0\zeta_0\dfrac{f_{13}f_{33} - f_{14}f_{34}}{f_{33}f_M} \\ \dfrac{B_1}{\sqrt{A_1}} = \dfrac{h_0(f_{12}f_{33} + f_{14}f_{13}) + \zeta_0(f_{13}f_{34} - f_{14}f_{33})}{\sqrt{f_{33}f_M(f_{11}f_{33} - f_{13}^2)}} \\ \sqrt{A_1} = \sqrt{\dfrac{f_{11}f_{33} - f_{13}^2}{f_{33}f_M}} \end{cases}$
Smith function $G_W(\nu, h_0, y_t, y_0)$	$-\ln\left[\dfrac{1 - \operatorname{erfc}(h_0 + y_t\nu\eta)/2}{1 - \operatorname{erfc}(h_0 + y_0\nu\eta)/2}\right]^{\Lambda(\nu)}$

where $G_{W,S}$ is obtained from (30), which is independent of ζ_0 and is given in table 1. For a normalized infinite observation length y_0, it becomes with a Gaussian process

$$\begin{aligned} G_W(\nu, h_0, y_t) &= \Lambda(\nu)\operatorname{erfc}(h_0 + y_t\nu\eta)/2 \\ G_S(\nu, h_0, y_t) &= -\ln[1 - \operatorname{erfc}(h_0 + y_t\nu\eta)/2]^{\Lambda(\nu)}. \end{aligned} \tag{32}$$

The substitution of (31) into (1) with variable transformations (29) leads to the following Wagner and Smith statistical shadowing functions:

$$S_{W,S}(\nu, h_0, \zeta_0, y_0) = \Upsilon(\nu - \zeta_0)\exp\left[-L_c\int_0^{y_t} g_{W,S}(\nu, h_0, \zeta_0, y)\,dy - G_{W,S}(\nu, h_0, y_t, y_0)\right]. \tag{33}$$

The above equation is valid whatever the surface height autocorrelation function which gives the value of y_t.

The uncorrelated case is similar, taking $f_{ij} = \delta_{ij}\ \forall y$ plotted in the full curve in figure 4, meaning that g expressed from (30) is valid for any y. Thus, the use of G given in table 1 with $y_t = 0$ means that the uncorrelated statistical shadowing function is

$$\begin{aligned} S_W(\nu, h_0, \zeta_0, y_0) &= \Upsilon(\nu - \zeta_0)\exp\left\{-\frac{\Lambda(\nu)}{2}[\operatorname{erf}(h_0 + y_0\nu\eta) - \operatorname{erf}(h_0)]\right\} \\ S_S(\nu, h_0, \zeta_0, y_0) &= \Upsilon(\nu - \zeta_0)\left[\frac{1 - \operatorname{erfc}(h_0)/2}{1 - \operatorname{erfc}(h_0 + y_0\nu\eta)/2}\right]^{\Lambda(\nu)}. \end{aligned} \tag{34}$$

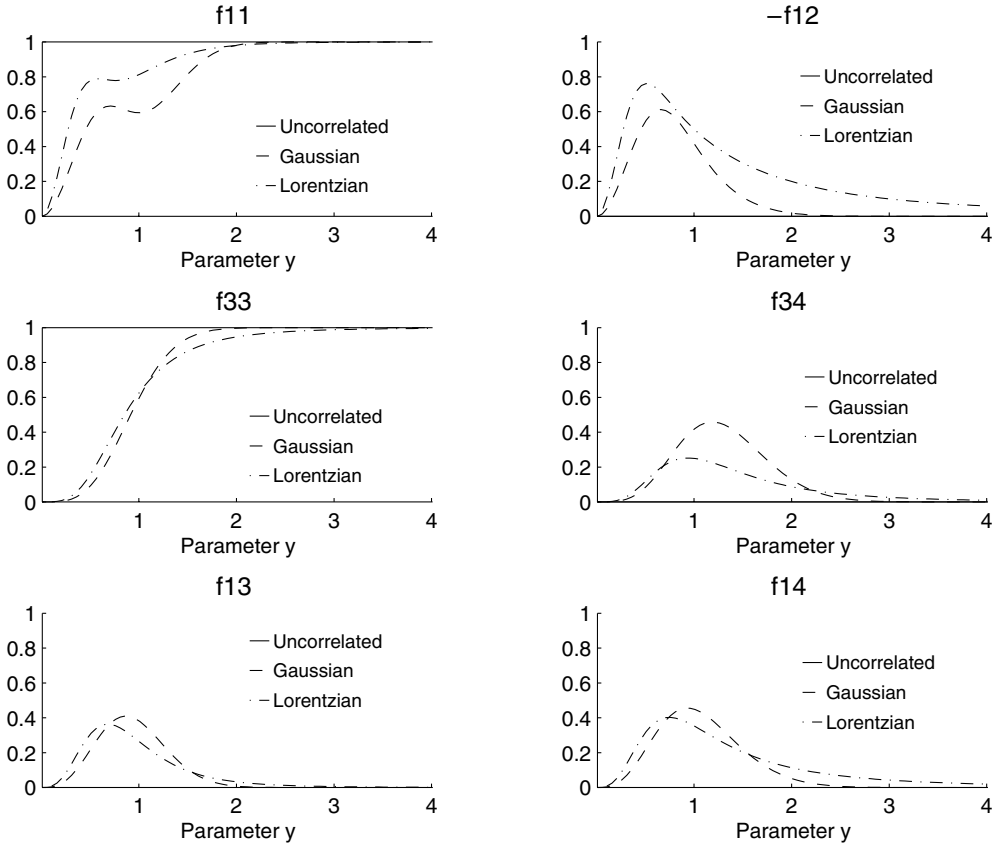

Figure 4. Functions $\{f_{ij}\}$ for Gaussian (broken curve) and Lorentzian (chain curve) surface height autocorrelation functions versus y. In the full curve, the uncorrelated case is plotted.

Table 2. Expressions of $R_{0,1,2}$ and $f_{0,1,2}$ for Gaussian and Lorentzian surface height autocorrelation functions.

	R_0 and f_0 functions	R_1 and f_1 functions	R_2 and f_2 functions	Slope rms σ
Gaussian	$R_0 = \omega^2 \exp\left(-\frac{l^2}{L_c^2}\right)$	$R_1 = -\frac{2l\omega^2}{L_c^2} \exp\left(-\frac{l^2}{L_c^2}\right)$	$R_2 = -\frac{2\omega^2}{L_c^2}\left(1 - 2\frac{l^2}{L_c^2}\right)\exp\left(-\frac{l^2}{L_c^2}\right)$	$\sigma = \omega\sqrt{2}/L_c$
	$f_0 = \exp(-y^2)$	$f_1 = y\sqrt{2}\exp(-y^2)$	$f_2 = (1 - 2y^2)\exp(-y^2)$	$\eta = \frac{\sigma L_c}{\omega} = \sqrt{2}$
Lorentzian	$R_0 = \omega^2 \Big/ \left(1 + \frac{l^2}{L_c^2}\right)$	$R_1 = -\frac{2l\omega^2}{L_c^2} \Big/ \left(1 + \frac{l^2}{L_c^2}\right)^2$	$R_2 = -\frac{2\omega^2}{L_c^2}\left(1 - 3\frac{l^2}{L_c^2}\right) \Big/ \left(1 + \frac{l^2}{L_c^2}\right)^3$	$\sigma = \omega\sqrt{2}/L_c$
	$f_0 = 1/(1 + y^2)$	$f_1 = y\sqrt{2}/(1 + y^2)^2$	$f_2 = (1 - 3y^2)/(1 + y^2)^3$	$\eta = \frac{\sigma L_c}{\omega} = \sqrt{2}$

For a normalized infinite observation length y_0, the second right-hand side terms of (34) are similar to (15) with $h_0 = \xi_0/(\omega\sqrt{2})$ and $\mathrm{erfc}(x) = 1 - \mathrm{erf}(x)$.

3.2. Simulations of the surface height and slope marginal cumulative functions

In this subsection, the shadowed probability density (2), assumed to be Gaussian, defined as

$$p_{\mathrm{Sh}}(\nu, h_0, \zeta_0) = \exp(-h_0^2 - \zeta_0^2) \times S_{\mathrm{W,S}}(\nu, h_0, \zeta_0)/\pi, \tag{35}$$

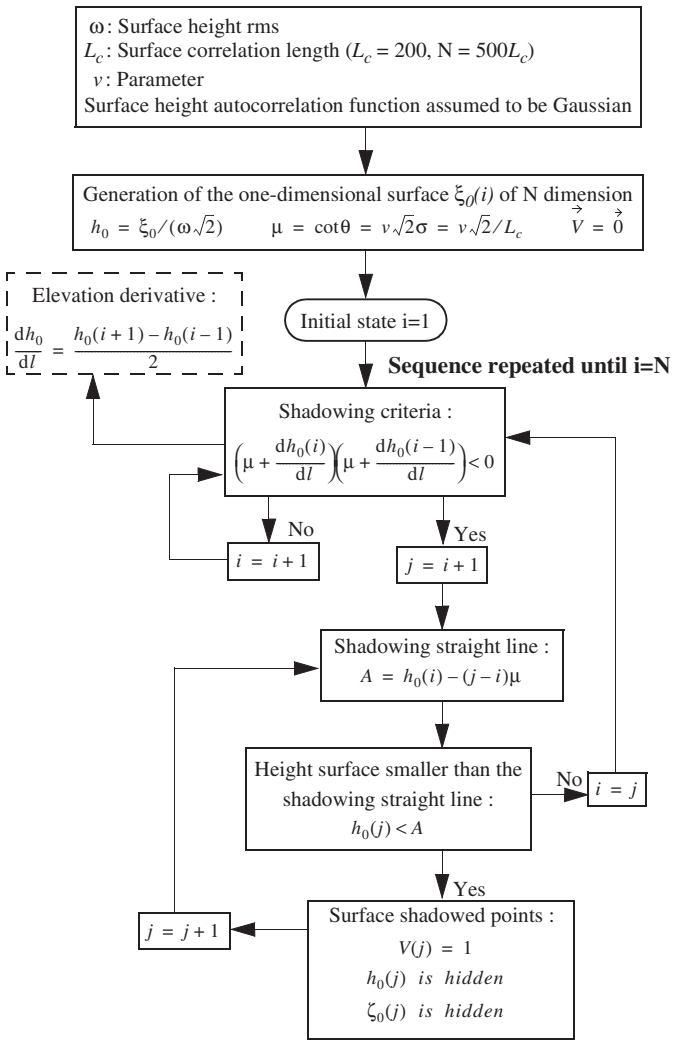

Figure 5. Explanation of the algorithm for computing the numerical monostatic statistical shadowing function. The vector $\vec{V}$ is used for the bistatic configuration.

is studied for an infinite observation length. The effect of the observation length will be investigated in the next paper. For uncorrelated and correlated Gaussian processes, the statistical shadowing functions $S_{W,S}(\nu, h_0, \zeta_0)$ are expressed from (34) and (33), respectively. With (33), the integration of $g_{W,S}$ over y is computed numerically.

To keep the formulation as accurate as possible, the different approaches are compared with the numerical statistical shadowing function obtained from the algorithm developed by Brokelman and Hagfors [13]. This algorithm is explained in figure 5. The surface height is generated by computing the convolution product of the filter coefficients by a Gaussian white noise with zero mean and unit height variance. Article [15] gives the method for performing the coefficient filter with a Gaussian surface height autocorrelation function.

To illustrate the algorithm, at the top of figure 6, using the broken curve, the shadowed surface height is plotted versus the sample indices and the parameter ν for both the Gaussian

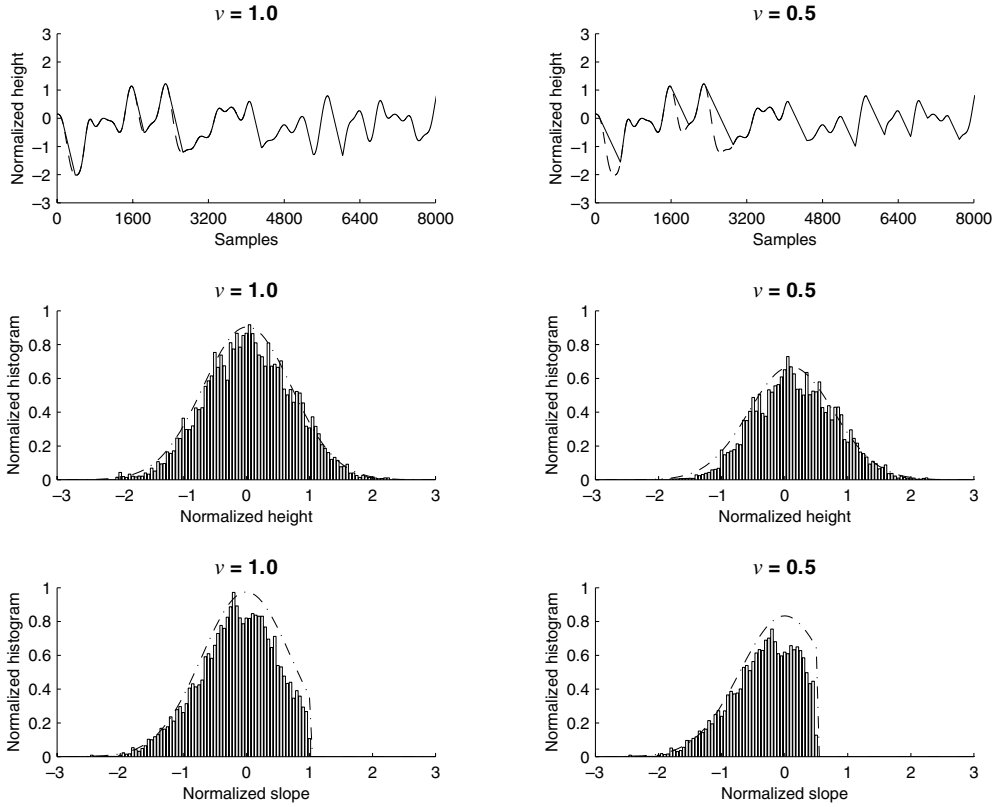

Figure 6. Top: the broken curve shows the shadowed surface height plotted versus the sample indices and the parameter ν for both the Gaussian surface height autocorrelation function and the process with zero mean and unit variance. The full curve represents the unshadowed surface and shadowing line. The surface correlation length $L_c = 200$ and the number of surface samples is $N = 500L_c$. Middle: the Smith uncorrelated surface height marginal pdf (chain curve) is compared with the shadowed surface-height-normalized histogram (full curve) versus the normalized height $h_0 = \xi_0/(\omega\sqrt{2})$. Bottom: the marginal probability over the slopes versus the normalized slopes $\zeta_0 = \gamma_0/(\sigma\sqrt{2})$.

surface height autocorrelation function and the process with zero mean and unit variance ($\omega = 1$). The full curve represents the unshadowed surface and shadowing line. The surface correlation length is $L_c = 200$ and the number of surface samples is $N = 500L_c$. We can observe that the number of shadowed points increases when $\nu = \cot\theta/(\sigma\sqrt{2})$ decreases because either the incidence angle increases or the surface is rougher.

In the middle, the Smith uncorrelated marginal surface height pdf (chain curve) is compared with the shadowed surface normalized histogram (full curve) versus the normalized height $h_0 = \xi_0/(\omega\sqrt{2})$. At the bottom the marginal probability over the slopes is plotted versus the normalized slopes $\zeta_0 = \gamma_0/(\sigma\sqrt{2})$. The surface height $p_{\mathrm{Sh}}(\nu, h_0)$ and slope $p_{\mathrm{Sh}}(\nu, \zeta_0)$ marginal pdfs are defined as

$$p_{\mathrm{Sh}}(\nu, h_0) = \int_{-\infty}^{\infty} p_{\mathrm{Sh}}(\nu, h_0, \zeta_0)\,\mathrm{d}\zeta_0 \qquad p_{\mathrm{Sh}}(\nu, \zeta_0) = \int_{-\infty}^{\infty} p_{\mathrm{Sh}}(\nu, h_0, \zeta_0)\,\mathrm{d}h_0. \tag{36}$$

Substituting (34) (uncorrelated case) into (35), the integrations over ζ_0 and h_0 with $y_0 = \infty$ yield

$$\text{Wagner}: \begin{cases} p_{\mathrm{Sh,W}}(\nu, h_0) = \Lambda_1 \times \exp(-h_0^2)\exp[-\Lambda \mathrm{erfc}(h_0)/2]/\sqrt{\pi} \\ p_{\mathrm{Sh,W}}(\nu, \zeta_0) = \Upsilon(\nu - \zeta_0)\exp(-\zeta_0^2)[1 - \exp(-\Lambda)]/(\Lambda\sqrt{\pi}), \end{cases} \tag{37}$$

$$\text{Smith}: \begin{cases} p_{\mathrm{Sh,S}}(\nu, h_0) = \Lambda_1 \times \exp(-h_0^2)[1 - \mathrm{erfc}(h_0)/2]^{\Lambda(\nu)}/\sqrt{\pi} \\ p_{\mathrm{Sh,S}}(\nu, \zeta_0) = \Upsilon(\nu - \zeta_0)\exp(-\zeta_0^2)/[(1 + \Lambda)\sqrt{\pi}], \end{cases} \tag{38}$$

where $\Lambda_1(\nu) = [1 + \mathrm{erf}(\nu)]/2$ and $\Lambda(\nu)$ given by (16). $p_{\mathrm{Sh}}(\nu, h_0, \zeta_0)$ cannot be computed numerically according to $\{h_0, \zeta_0\}$ because the shadowing effect involves two conditions over the surface slopes and heights. Moreover, this allows us to reduce the number of variables by one, which facilitates the interpretation of the results. The normalized histogram is obtained from the maximum of the unshadowed histogram. As shown in figure 6, there is a good agreement between the numerical and Smith uncorrelated results.

At the top of figure 7, the Wagner (broken curve), Smith (chain curve) and numerical (full curve) marginal cumulative functions over the surface heights in the uncorrelated case are plotted versus the normalized heights h_{01}. On the bottom, they are over the surface slopes versus the normalized slopes ζ_{01}. The marginal cumulative functions are defined as

$$\text{over the surface heights: } F(\nu, h_{01}) = \int_{-\infty}^{h_{01}} p_{\mathrm{Sh}}(\nu, h_0)\,\mathrm{d}h_0 = \int_{-\infty}^{h_{01}} \mathrm{d}h_0 \left[\int_{-\infty}^{\infty} p_{\mathrm{Sh}}(\nu, h_0, \zeta_0)\,\mathrm{d}\zeta_0\right], \tag{39}$$

$$\text{over the surface slopes: } F(\nu, \zeta_{01}) = \int_{-\infty}^{\zeta_{01}} p_{\mathrm{Sh}}(\nu, \zeta_0)\,\mathrm{d}\zeta_0 = \int_{-\infty}^{\zeta_{01}} \mathrm{d}\zeta_0 \left[\int_{-\infty}^{\infty} p_{\mathrm{Sh}}(\nu, h_0, \zeta_0)\,\mathrm{d}h_0\right]. \tag{40}$$

Substituting (37) and (38) into (39) and (40), we have in the uncorrelated case

$$\text{Wagner}: \begin{cases} F_{\mathrm{W}}(\nu, h_{01}) = \dfrac{\Lambda_1}{\Lambda}\{\exp[-\Lambda \mathrm{erfc}(h_{01})/2] - \exp(-\Lambda)\} \\ F_{W}(\nu, \zeta_{01}) = \dfrac{1 - \exp(-\Lambda)}{\Lambda} \begin{cases} [1 + \mathrm{erf}(\zeta_{01})]/2 & \text{if} \quad \zeta_{01} \leqslant \nu \\ \Lambda_1 & \text{otherwise,} \end{cases} \end{cases} \tag{41}$$

$$\text{Smith}: \begin{cases} F_{\mathrm{S}}(\nu, h_{01}) = \dfrac{\Lambda_1}{1 + \Lambda}[1 - \mathrm{erfc}(h_{01})/2]^{1+\Lambda} \\ F_{\mathrm{S}}(\nu, \zeta_{01}) = \dfrac{1}{1 + \Lambda} \begin{cases} [1 + \mathrm{erf}(\zeta_{01})]/2 & \text{if} \quad \zeta_{01} \leqslant \nu \\ \Lambda_1 & \text{otherwise.} \end{cases} \end{cases} \tag{42}$$

We can note $F(\nu, h_{01} = \infty) = F(\nu, \zeta_{01} = \infty)$, which is equal to the average monostatic shadowing function given by (18). As shown in figure 7, the uncorrelated Smith results are more accurate than the Wagner ones, and the discrepancy between the Smith and numerical data weakly increases when ν decreases.

In figure 8, the absolute differences of the Wagner (the broken curve in the uncorrelated case and the crosses in the correlated case) and Smith (the chain curve in the uncorrelated case and the circles in the correlated case) marginal cumulative functions from that obtained numerically are plotted.

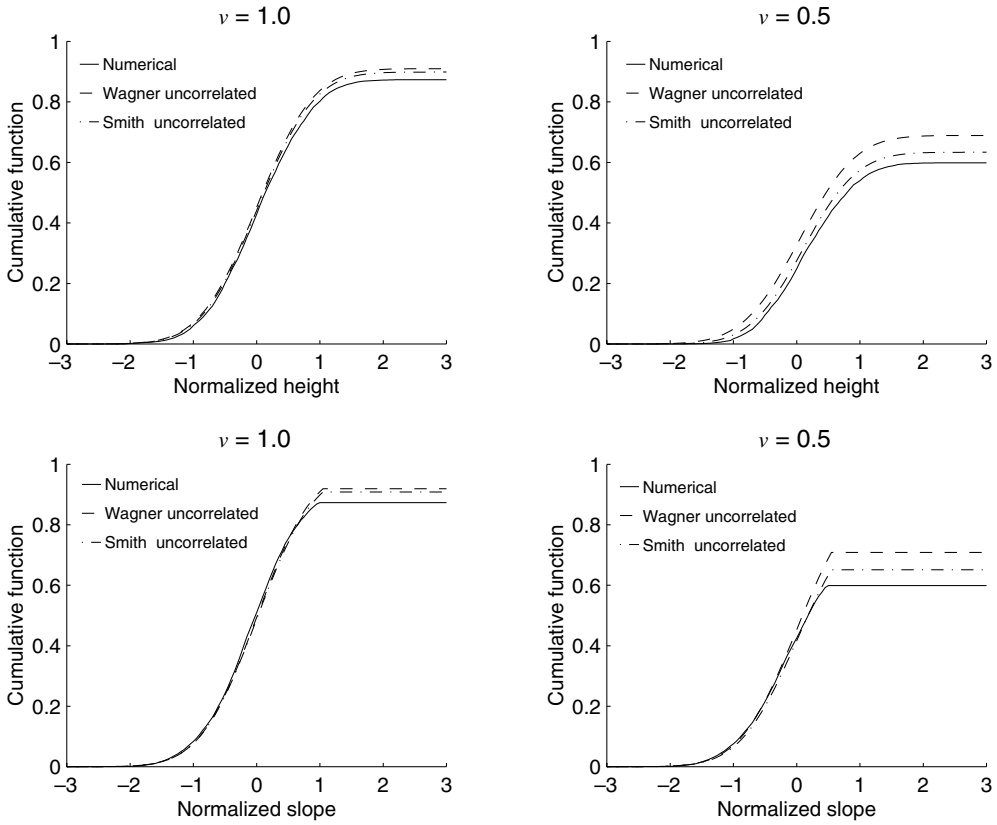

Figure 7. Top: the Wagner (broken curve), Smith (chain curve) and numerical (full curve) marginal cumulative functions over the surface slopes in the uncorrelated case are plotted versus the normalized heights h_{01}. Bottom: they are over the surface slopes versus the normalized slopes ζ_{01}.

The marginal cumulative functions with correlation are computed by using (33), (35), (36), (39) and (40) with $y_0 = \infty$ and $y_t = 3$ (for a Gaussian surface height autocorrelation function). We show that

$$F_{\mathrm{W,S}}(\nu, \zeta_{01}) = \frac{1}{\pi} \int_{-\infty}^{\text{if } \zeta_{01} < \nu} \exp(-\zeta_0^2)\, \mathrm{d}\zeta_0 \left\{ \int_{-\infty}^{\infty} \exp\left[- L_{\mathrm{c}} \int_0^{y_t} g_{\mathrm{W,S}}(\nu, h_0, \zeta_0, y)\, \mathrm{d}y \right.\right.$$
$$\left.\left. - G_{\mathrm{W,S}}(\nu, h_0, y_t) \right] \exp(-h_0^2)\, \mathrm{d}h_0 \right\} \qquad \text{else } F_{\mathrm{W,S}}(\nu, \nu), \tag{43}$$

$$F_{\mathrm{W,S}}(\nu, h_{01}) = \frac{1}{\pi} \int_{-\infty}^{h_{01}} \exp(-h_0^2)\, \mathrm{d}h_0 \left\{ \int_{-\infty}^{\nu} \exp\left[- L_{\mathrm{c}} \int_0^{y_t} g_{\mathrm{W,S}}(\nu, h_0, \zeta_0, y)\, \mathrm{d}y \right.\right.$$
$$\left.\left. - G_{\mathrm{W,S}}(\nu, h_0, y_t) \right] \exp(-\zeta_0^2)\, \mathrm{d}\zeta_0 \right\}, \tag{44}$$

where $L_{\mathrm{c}} g_{\mathrm{W,S}}(\nu, h_0, \zeta_0, y)$ and $G_{\mathrm{W,S}}(\nu, h_0, y_t)$ are expressed in table 1 and (32), respectively.

As seen in figure 8, the correlation slightly improves the results and the Smith results remain better than Wagner's. According to the numerical solution, the Smith and Wagner data overestimated the shadow.

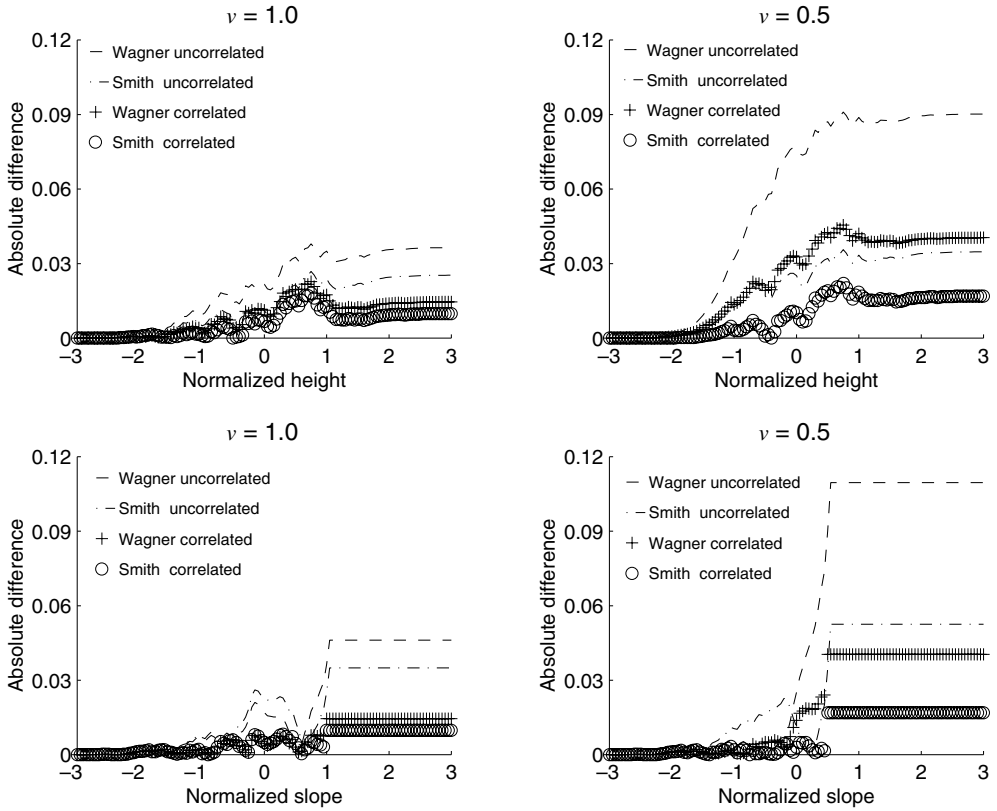

Figure 8. Absolute differences of the Wagner (broken curve in the uncorrelated case and crosses in the correlated case) and Smith (chain curve in the uncorrelated case and circles in the correlated case) marginal cumulative functions from that obtained numerically.

In figure 9, the numerical monostatic height and slope marginal cumulative functions are plotted versus the parameter ν and the normalized heights h_{01} and slopes ζ_{01}, respectively. They are also compared (within the absolute difference) with those obtained from the Smith uncorrelated and correlated approaches. We observe that the correlation improves the model.

In figure 10, the monostatic average shadowing function is plotted versus the parameter ν: full curve, the numerical solution computed for a Gaussian surface height autocorrelation function; crosses, the uncorrelated Smith solution ((18) with $\Lambda_1(\nu) = [1 + \mathrm{erf}(\nu)]/2$ and $\Lambda(\nu)$ given by (16)); broken and chain curves, the Smith correlated solution for Gaussian and Lorentzian surface height autocorrelation functions, respectively. It is defined as

$$\frac{1}{\pi}\int_{-\infty}^{\infty}\exp(-h_0^2)\,\mathrm{d}h_0\left\{\int_{-\infty}^{\nu}\exp\left[-L_c\int_0^{y_t}g_{W,S}(\nu,h_0,\zeta_0,y)\,\mathrm{d}y\right.\right.$$
$$\left.\left.-G_{W,S}(\nu,h_0,y_t)\right]\exp(-\zeta_0^2)\,\mathrm{d}\zeta_0\right\}, \tag{45}$$

where $L_c g_{W,S}(\nu,h_0,\zeta_0,y)$ and $G_{W,S}(\nu,h_0,y_t)$ are expressed in table 1 and (32), respectively.

From table 2, for Gaussian and Lorentzian surface heights autocorrelation functions, the surface slope rms σ is similar, which means that the Smith uncorrelated average shadowing function is also similar since it depends only on $\nu = \mu/(\sigma\sqrt{2})$. Unlike the case shown

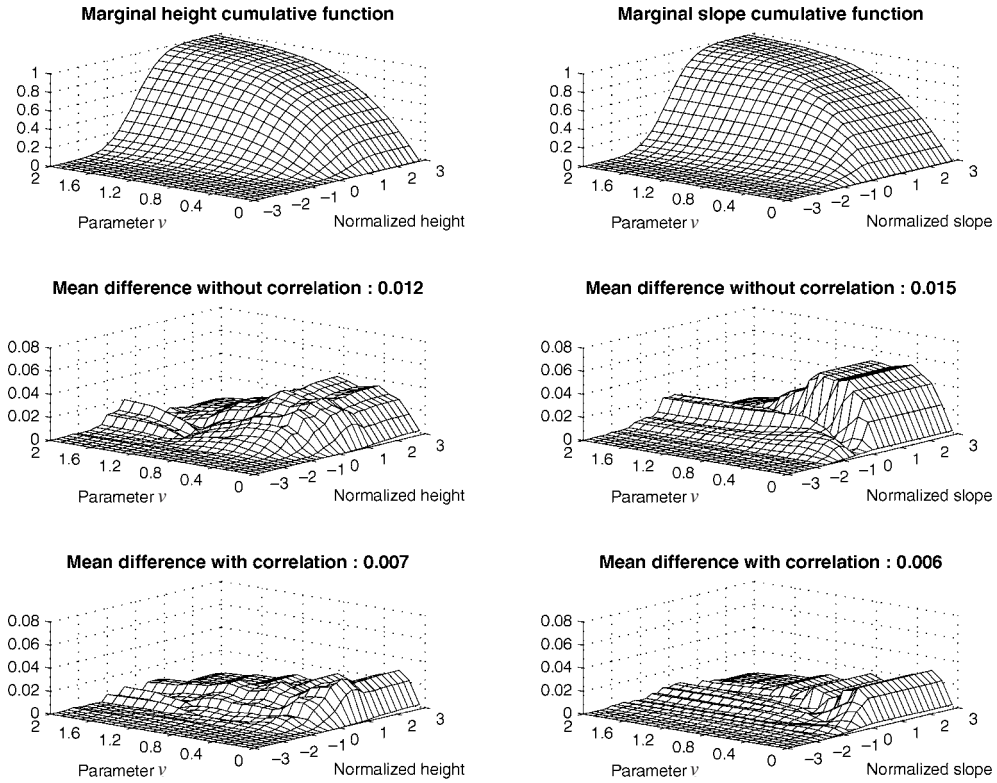

Figure 9. Top: numerical height and slope monostatic marginal cumulative functions versus the parameter v, and the normalized heights h_{01} and slopes ζ_{01}, respectively. Middle: the absolute difference between the Smith function without correlation and numerical results. Bottom: the absolute difference between the Smith function with correlation and numerical results.

in figure 4, with correlation it differs because the terms f_{ij} are not equal for each case. This effect is illustrated in figure 10, and we can note that the deviation between the Gaussian and Lorentzian solutions is weak.

4. Extension to a bistatic configuration

This section presents the uncorrelated and correlated bistatic statistical shadowing functions for a one-dimensional rough surface. Since the results obtained with the Smith formulation are more accurate than Wagner's, only the Smith approach is kept in the following.

4.1. Statistical shadowing function without correlation

From equation (2.31) of [14], the statistical bistatic shadowing function is given by (figures 11 and 12)

$$S(\mu_1, \mu_2, F, L_0) = \begin{cases} S(\mu_1, F, L_0)S(\mu_2, F, L_0) & \text{if } \theta_2 \in [0; \pi/2] \quad \text{case } (a) \\ S(\mu_1, F, L_0) & \text{if } \theta_2 \in [\theta_1; 0[\quad \text{case } (b) \\ S(\mu_2, F, L_0) & \text{if } \theta_2 \in [-\pi/2; \theta_1[\quad \text{case } (c), \end{cases} \tag{46}$$

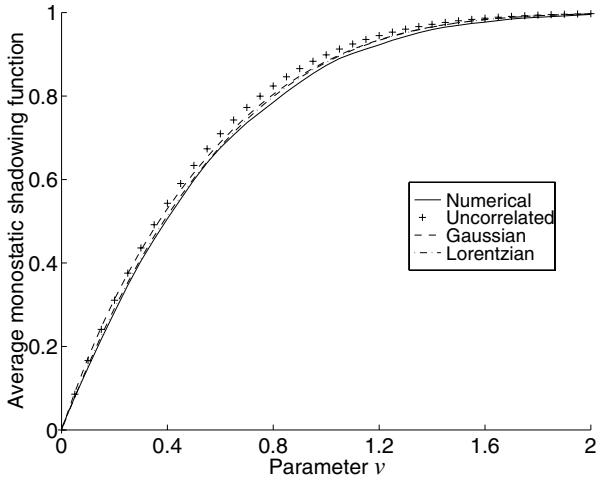

Figure 10. Monostatic average shadowing function versus the parameter v. Full curve, the numerical solution computed for a Gaussian surface height autocorrelation function. Crosses, the uncorrelated Smith solution. Broken and chain curves, the Smith correlated solutions for Gaussian and Lorentzian autocorrelation functions, respectively.

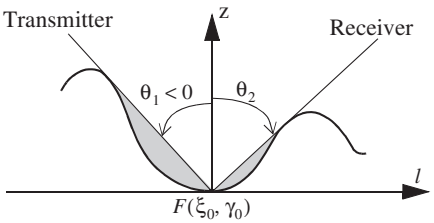

Figure 11. Bistatic statistical shadowing function.

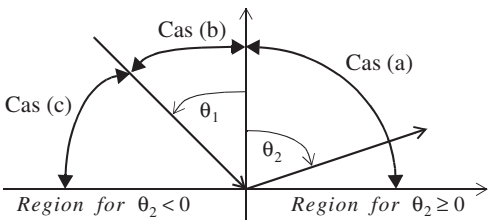

Figure 12. Geometric representation of the three cases for the bistatic configuration.

with $\theta_1 \leqslant 0$. Equation (46) means that the statistical bistatic shadowing function $S(\mu_1, \mu_2, F, L_0)$ is obtained from two independent statistical monostatic shadowing functions defined with respect to the locations of the transmitter $S(\mu_1, F, L_0)$ and receiver $S(\mu_2, F, L_0)$. Consequently the (b) and (c) cases are similar to the monostatic configuration, and case (a) has to be investigated.

Using (12) with (12*b*), the Smith (*a*) case of (46) for an uncorrelated process is expressed as

$$S_{\mathrm{S}}(\mu_1, F, L_0)S_{\mathrm{S}}(\mu_2, F, L_0) = \Upsilon(|\mu_1| + \gamma_0)\left[\frac{P(\xi_0) - P(-\infty)}{P(\xi_0 + |\mu_1|L_0) - P(-\infty)}\right]^{\Lambda(\nu_1)} \times \Upsilon(\mu_2 - \gamma_0)\left[\frac{P(\xi_0) - P(-\infty)}{P(\xi_0 + \mu_2 L_0) - P(-\infty)}\right]^{\Lambda(\nu_2)}, \tag{47}$$

with

$$\nu_i = |\mu_i|/(\sigma\sqrt{2}). \tag{48}$$

Since the transmitter is defined for $l < 0$, the sign of γ_0 in $\Upsilon(|\mu_1| + \gamma_0)$ is positive and the slope $\mu_1 = \cot\theta_1$ of the incident ray becomes $|\mu_1|$. Therefore, with variable transformations (29), (46) becomes

$$S_{\mathrm{S}}(\nu_1, \nu_2, h_0, \zeta_0, y_0) = \begin{cases} \Pi\left[\dfrac{P(h_0) - P(-\infty)}{P(h_0 + \nu_1\eta y_0) - P(-\infty)}\right]^{\Lambda(\nu_1)} \\ \quad \times \left[\dfrac{P(h_0) - P(-\infty)}{P(h_0 + \nu_2\eta y_0) - P(-\infty)}\right]^{\Lambda(\nu_2)} & \text{if} \quad \nu_2 \geqslant 0 \\ \Upsilon(\nu_2 - \zeta_0)\left[\dfrac{P(\xi_0) - P(-\infty)}{P(h_0 + \nu_2\eta y_0) - P(-\infty)}\right]^{\Lambda(\nu_2)} \\ \qquad \text{if} \quad -\nu_1 \leqslant -\nu_2 < 0 \\ \Upsilon(\nu_1 - \zeta_0)\left[\dfrac{P(\xi_0) - P(-\infty)}{P(h_0 + \nu_1\eta y_0) - P(-\infty)}\right]^{\Lambda(\nu_1)} \\ \qquad \text{if} \quad -\infty \leqslant -\nu_2 < -\nu_1, \end{cases} \tag{49}$$

with

$$\Pi = \begin{cases} 1 & \text{if} \quad \zeta_0 \in [-\nu_1; \nu_2] \\ 0 & \text{else.} \end{cases} \tag{49a}$$

Consequently, using (2) with a Gaussian uncorrelated process (in (49) P is expressed from (14)) and an infinite observation length, the surface height and slope distributions with shadow are

$$p_{\mathrm{Sh}}(\nu_1, \nu_2, h_0, \zeta_0) = \begin{cases} \dfrac{1}{\sqrt{\pi}}\Pi\exp(-\zeta_0^2) \times \dfrac{1}{\sqrt{\pi}}\exp(-h_0^2)\left[1 - \dfrac{1}{2}\mathrm{erfc}(h_0)\right]^{\Lambda(\nu_1)+\Lambda(\nu_2)} \\ \qquad \text{if} \quad \nu_2 \geqslant 0 \\ \dfrac{1}{\sqrt{\pi}}\Upsilon(\nu_2 - \zeta_0)\exp(-\zeta_0^2) \times \dfrac{1}{\sqrt{\pi}}\exp(-h_0^2)\left[1 - \dfrac{1}{2}\mathrm{erfc}(h_0)\right]^{\Lambda(\nu_2)} \\ \qquad \text{if} \quad -\nu_1 \leqslant -\nu_2 < 0 \\ \dfrac{1}{\sqrt{\pi}}\Upsilon(\nu_1 - \zeta_0)\exp(-\zeta_0^2) \times \dfrac{1}{\sqrt{\pi}}\exp(-h_0^2)\left[1 - \dfrac{1}{2}\mathrm{erfc}(h_0)\right]^{\Lambda(\nu_1)} \\ \qquad \text{if} \quad -\infty \leqslant -\nu_2 < -\nu_1. \end{cases} \tag{50}$$

In figure 13, the shadowed bistatic distributions of the surface slopes (left) and heights (right) are plotted according to the parameter ν_2 and versus the normalized surface slopes $\zeta_0 = \gamma_0/(\sigma\sqrt{2})$ and heights $h_0 = \xi_0/(\omega\sqrt{2})$ for a given ν_1. Since $\nu_1 < 0$, only the first case (*a*) of figure 13 is studied. For the slope distribution, the Π function carries a restriction over the surface slopes meaning that only the slopes contained in the range $\zeta_0 \in [-\nu_1; \nu_2]$ are taken into account. On the right, we can see that the height distribution is non-Gaussian, with a maximum which decreases when $\{|\nu_1|, \nu_2\}$ decrease.

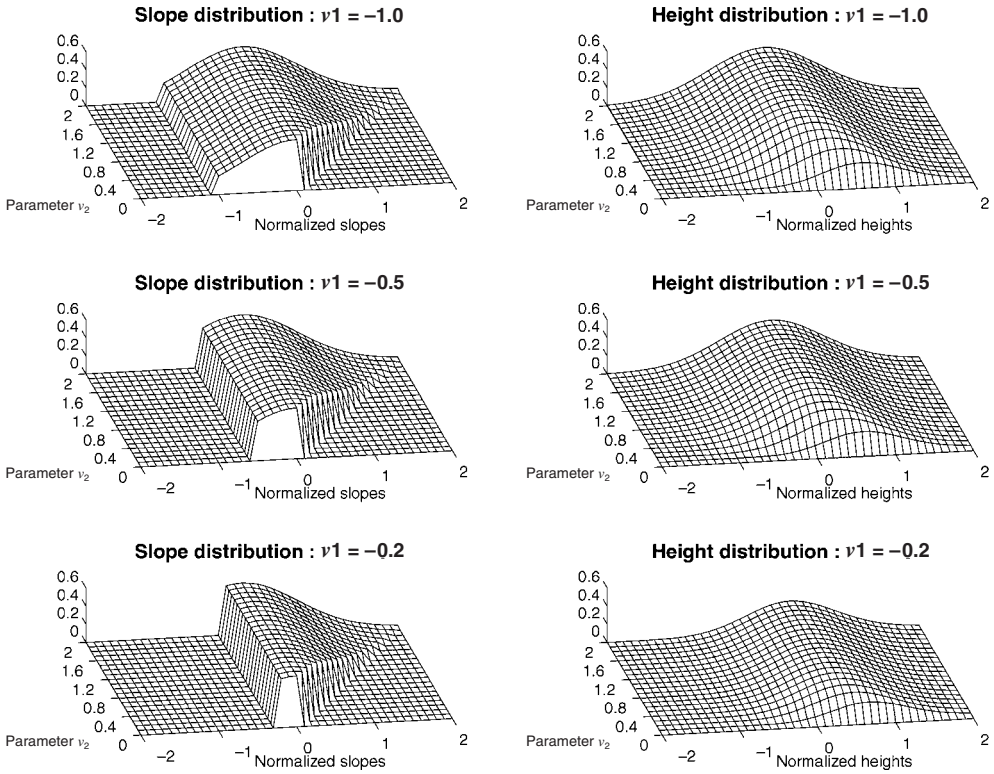

Figure 13. Shadowed bistatic distributions of the surface slopes (left) and heights (right) according to the parameter ν_2 and versus the normalized surface slopes $\zeta_0 = \gamma_0/(\sigma\sqrt{2})$ and heights $h_0 = \xi_0/(\omega\sqrt{2})$ for given ν_1.

4.2. Numerical solution and statistical shadowing function with correlation

For a Gaussian correlated process, we obtained from (33) and table 1

$$S_S(\nu_1, \nu_2, h_0, \zeta_0, y_0) = \begin{cases} \Pi \times \exp\left[-L_c \displaystyle\int_0^{y_t} g_{S12}(\nu_1, \nu_2, h_0, \zeta_0, y)\,\mathrm{d}y\right] \\ \quad \times \left[\dfrac{1-\operatorname{erfc}(h_0 + y_t\nu_1\eta)/2}{1-\operatorname{erfc}(h_0 + y_0\nu_1\eta)/2}\right]^{\Lambda(\nu_1)} \left[\dfrac{1-\operatorname{erfc}(h_0 + y_t\nu_2\eta)/2}{1-\operatorname{erfc}(h_0 + y_0\nu_2\eta)/2}\right]^{\Lambda(\nu_2)} \\ \qquad \text{if} \quad \boldsymbol{\nu}_2 \geqslant \mathbf{0} \\ \Upsilon(\nu_2 - \zeta_0)\exp\left[-L_c \displaystyle\int_0^{y_t} g_S(\nu_2, h_0, \zeta_0, y)\,\mathrm{d}y\right] \\ \quad \times \left[\dfrac{1-\operatorname{erfc}(h_0 + y_t\nu_2\eta)/2}{1-\operatorname{erfc}(h_0 + y_0\nu_2\eta)/2}\right]^{\Lambda(\nu_2)} \qquad \text{if} \quad -\boldsymbol{\nu}_1 \leqslant -\boldsymbol{\nu}_2 < 0 \\ \Upsilon(\nu_1 - \zeta_0)\exp\left[-L_c \displaystyle\int_0^{y_t} g_S(\nu_1, h_0, \zeta_0, y)\,\mathrm{d}y\right] \\ \quad \times \left[\dfrac{1-\operatorname{erfc}(h_0 + y_t\nu_1\eta)/2}{1-\operatorname{erfc}(h_0 + y_0\nu_1\eta)/2}\right]^{\Lambda(\nu_1)} \qquad \text{if} \quad -\infty \leqslant -\boldsymbol{\nu}_2 < -\boldsymbol{\nu}_1, \end{cases} \tag{51}$$

with

$$g_{S12}(\nu_1, \nu_2, h_0, \zeta_0, y) = g_S(\nu_1, h_0, \zeta_0, y) + g_S(\nu_2, h_0, \zeta_0, y). \tag{51a}$$

Since the (b) and (c) cases are monostatic, the numerical statistical shadowing function is computed from the algorithm of figure 5. For the (a) case this algorithm is used twice with the following method.

Let V_1 be a vector defined with respect to the emitter (subscript 1) as

$$V_1(i) = \begin{cases} 1 & \text{if the surface point } i \text{ is shadowed} \\ 0 & \text{else,} \end{cases} \tag{52}$$

and V_2 the same vector defined from the receiver. For a bistatic configuration, a point of the surface is hidden if it is not viewed by the receiver or the transmitter. The vector V_{12} for the (a) case is then expressed as

$$V_{12} = V_1 \oplus V_2, \tag{53}$$

where the symbol $\oplus$ denotes the OR logical operator. Since $\nu_1 \leqslant 0$ and $\nu_2 \geqslant 0$, the sign is distinguished by computing V_2 with the negative-height surface $-h_0(i)$. Thus, the vector which gives the unshadowed point is $\bar{V}_{12} = \bar{V}_1 \cdot \bar{V}_2$, with $^-$ and $\cdot$ the NOT and AND logical operators, respectively.

For an infinite observation length, from (35), (39) and (40) with the use of (50) and (51), the bistatic marginal cumulative function over the surface heights $F_S(\nu_1, \nu_2, h_{01})$ and slopes $F_S(\nu_1, \nu_2, \zeta_{01})$ in the (a) case for a Gaussian process are

$$\text{without correlation} \begin{cases} F_S(\nu_1, \nu_2, h_{01}) = \dfrac{\operatorname{erf}(\nu_1) + \operatorname{erf}(\nu_2)}{2[1 + \Lambda(\nu_1) + \Lambda(\nu_2)]} \times \left[1 - \dfrac{1}{2}\operatorname{erfc}(h_{01})\right]^{1+\Lambda(\nu_1)+\Lambda(\nu_2)} \\ F_S(\nu_1, \nu_2, \zeta_{01}) = \dfrac{1}{1 + \Lambda(\nu_1) + \Lambda(\nu_2)} \times \begin{cases} 0 & \text{if} \quad \zeta_{01} \leqslant -\nu_1 \\ [\operatorname{erf}(\nu_1) + \operatorname{erf}(\zeta_{01})]/2 & \text{if} \quad -\nu_1 < \zeta_{01} \leqslant \nu_2 \\ [\operatorname{erf}(\nu_1) + \operatorname{erf}(\nu_2)]/2 & \text{if} \quad \zeta_{01} > \nu_2, \end{cases} \end{cases} \tag{54}$$

$$\text{with correlation} \begin{cases} F_S(\nu_1, \nu_2, h_{01}) = \dfrac{1}{\pi} \displaystyle\int_{-\infty}^{h_{01}} \exp(-h_0^2) E_{12}(\nu_1, \nu_2, h_0)\, \mathrm{d}h_0 \\ \quad \times \left\{ \displaystyle\int_{-\nu_1}^{\nu_2} \exp\left[-L_c \int_0^{y_t} g_{S12}(\nu_1, \nu_2, h_0, \zeta_0, y)\, \mathrm{d}y \right] \exp(-\zeta_0^2)\, \mathrm{d}\zeta_0 \right\} \\ F_S(\nu_1, \nu_2, \zeta_{01}) = \begin{cases} 0 & \text{if} \quad \zeta_{01} \leqslant -\nu_1 \\ \dfrac{1}{\pi} \displaystyle\int_{-\nu_1}^{\zeta_{01}} \exp(-\zeta_0^2)\, \mathrm{d}\zeta_0 \\ \quad \times \left\{ \displaystyle\int_{-\infty}^{\infty} E_{12}(\nu_1, \nu_2, h_0) \exp(-h_0^2) \right. \\ \quad \left. \times \exp\left[-L_c \displaystyle\int_0^{y_t} g_{S12}(\nu_1, \nu_2, h_0, \zeta_0, y)\, \mathrm{d}y \right] \mathrm{d}h_0 \right\} \\ \qquad \text{if} \quad -\nu_1 < \zeta_{01} \leqslant \nu_2 \\ F_S(\nu_1, \nu_2, \nu_2) \\ \qquad \text{if} \quad \zeta_{01} > \nu_2 \end{cases} \end{cases} \tag{55}$$

with

$$E_{12}(\nu_1, \nu_2, h_0) = [1 - \tfrac{1}{2}\operatorname{erfc}(h_0 + y_t \nu_1 \eta)]^{\Lambda(\nu_1)} [1 - \tfrac{1}{2}\operatorname{erfc}(h_0 + y_t \nu_2 \eta)]^{\Lambda(\nu_2)}. \tag{55a}$$

At the top of figures 14 ($\nu_1 = -1$) and 15 ($\nu_1 = -0,5$), the numerical height and slope bistatic marginal cumulative functions are represented versus the parameter ν_2, and the normalized heights $h_0 = \xi_0/(\omega\sqrt{2})$ and slopes $\zeta_0 = \gamma_0/(\sigma\sqrt{2})$, respectively. In the middle is the

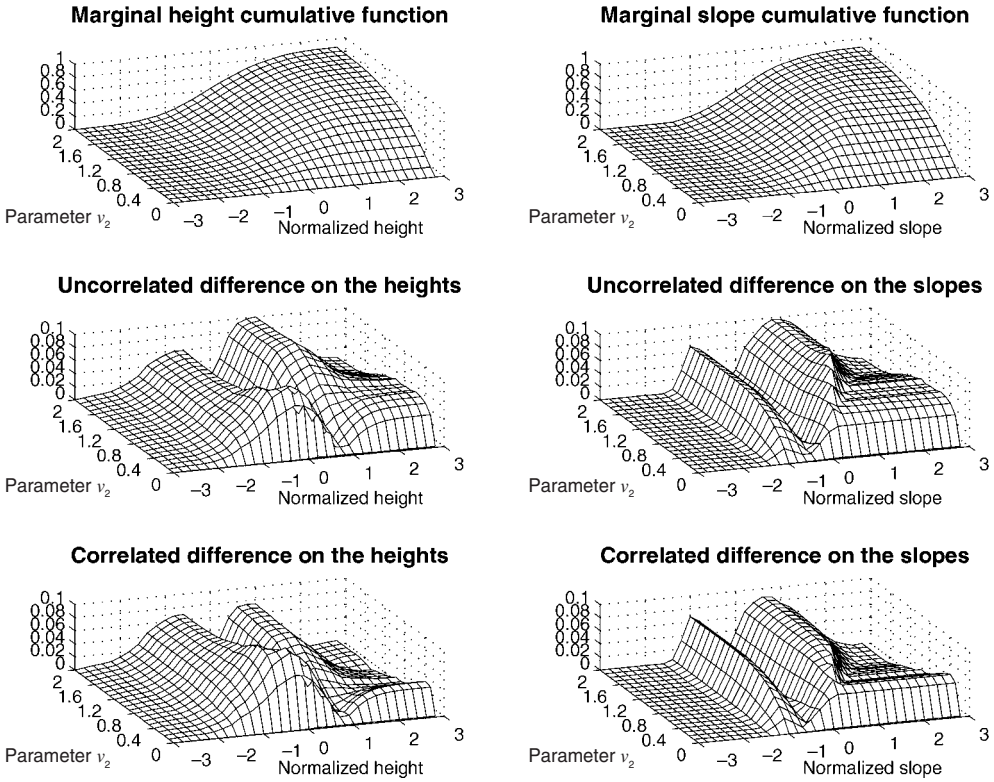

Figure 14. Top: numerical height and slope bistatic marginal cumulative functions versus the parameter v_2, and the normalized heights $h_0 = \xi_0/(\omega\sqrt{2})$ and slopes $\zeta_0 = \gamma_0/(\sigma\sqrt{2})$, respectively. Middle: the absolute difference between the Smith function without correlation and numerical results. Bottom: the absolute difference between the Smith function with correlation and numerical results. $|v_1| = 1$.

absolute difference between the Smith function without correlation and numerical results. At the bottom is the absolute difference between the Smith function with correlation and numerical results. As in the monostatic case, the deviation between the numerical and correlated data is slight, and with the uncorrelated results the difference is larger, but remains small.

5. Conclusion and discussion of the electromagnetic scattering problem

5.1. Conclusion

In this paper, with the Wagner and Smith formulations, the monostatic and bistatic statistical shadowing functions from a one-dimensional rough surface are presented for an uncorrelated process and for a given observation length. Since the correlation is assumed to be neglected, the statistical shadowing function does not depend on the surface height autocorrelation function. Although the Ricciardi–Sato function gives the exact solution, we have only studied it for an uncorrelated process, since with a correlated process it is not tractable analytically or numerically.

To study the correlation effect on the surface heights and slopes, the Gaussian process is investigated for any surface height autocorrelation function. For a monostatic configuration with an infinite observation length, the comparisons of the numerical solution, which uses no

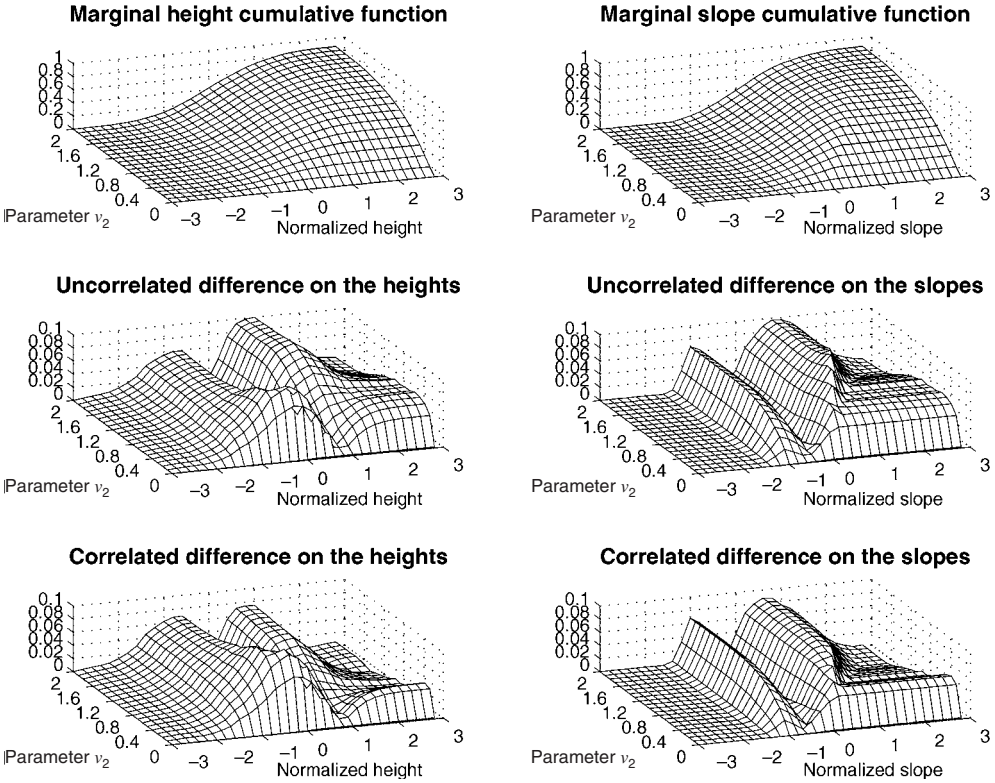

Figure 15. Top: numerical height and slope bistatic marginal cumulative functions versus the parameter v_2, and the normalized heights $h_0 = \xi_0/(\omega\sqrt{2})$ and slopes $\zeta_0 = \gamma_0/(\sigma\sqrt{2})$, respectively. Middle: the absolute difference between the Smith function without correlation and numerical results. Bottom: the absolute difference between the Smith function with correlation and numerical results. $|v_1| = 0.5$.

assumption, with the correlated and uncorrelated formulations show that the Smith approach is the most accurate. Moreover, the correlation weakly improves the model but the uncorrelated results remain satisfactory. According to the surface height autocorrelation function (Gaussian and Lorentzian), the average shadowing function varies weakly.

We have shown that the monostatic shadowing effect can be ignored if the parameter $v = \cot\theta/(\sigma\sqrt{2})$ is greater than $v_0 = 2$, corresponding to a limit incidence angle smaller than $\theta_0 = \operatorname{arc\,cot}(\sigma\sqrt{2}v_0)$ plotted in figure 16 versus the surface slope rms for $v_0 = \{2, 1.5\}$. For example if $\sigma = 0.2$, then the shadowing effect can be ignored if $\theta_0 \leqslant \{60^\circ, 68^\circ\}$ for $v_0 = \{2, 1.5\}$, respectively. For a bistatic configuration, we find similar conclusions, and the shadowing effect can be omitted if both $\{|v_1|, |v_2|\} \geqslant v_0$.

The computation of $L_c g_{W,S}(v, h_0, \zeta_0, y)$ expressed in table 1 implies numerical problems. To overcome them, the following expansions of $1 + \operatorname{erf}(x)$ and $1 - x\sqrt{\pi}\operatorname{erfc}(x)\exp(x^2)$ are used, respectively:

$$1 + \operatorname{erf}(x) = -1/[x\sqrt{\pi}\exp(x^2)] \qquad \text{for} \quad x < -5.6, \tag{56}$$

and

$$1 - x\sqrt{\pi}\operatorname{erfc}(x)\exp(x^2) = \begin{cases} 1/(2x^2) & \text{for} \quad x > 12.2 \\ -2x\sqrt{\pi}\exp(x^2) & \text{for} \quad x < -2.2. \end{cases} \tag{57}$$

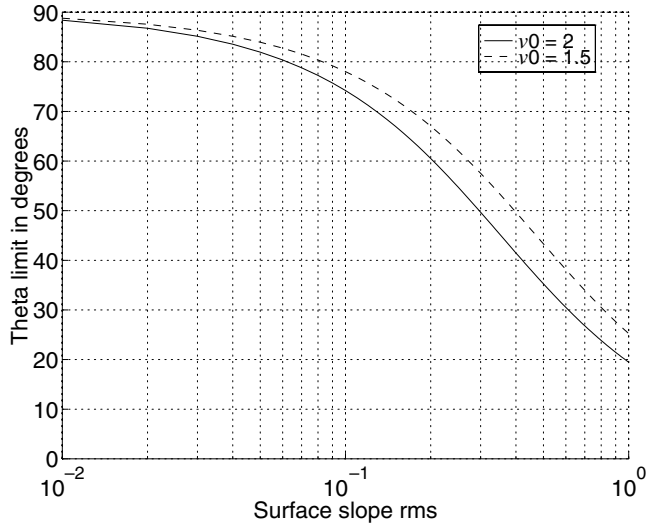

Figure 16. Theta limit angle versus the surface slope rms σ for a monostatic configuration.

Combining these equations with the exponential term of $g_{\mathrm{W,S}}$, the numerical problems are solved.

5.2. Discussion of the electromagnetic scattering problem

In the electromagnetic scattering problem from a rough surface, the scattering coefficient σ_{S} is obtained by averaging the scattered electromagnetic field of component E_{S} multiplied by its conjugate $E_{\mathrm{S}}^{*\prime}$

$$\sigma_{\mathrm{S}} = \langle E_{\mathrm{S}} E_{\mathrm{S}}^{*\prime} \rangle, \tag{58}$$

with $\langle \cdots \rangle$ the average operator. For example, if E_{S} depends on $\{\xi_0, \gamma_0\}$ and if the shadowing effect is included then

$$\sigma_{\mathrm{S}} = \int\int\int\int E_{\mathrm{S}}(\xi_0, \gamma_0) \times E_{\mathrm{S}}^{*}(\xi_0', \gamma_0') p_{\mathrm{Sh}}(\nu_1, \nu_2, \xi_0, \gamma_0, \xi_0', \gamma_0') \, \mathrm{d}\xi_0 \, \mathrm{d}\gamma_0 \, \mathrm{d}\xi_0' \, \mathrm{d}\gamma_0'. \tag{59}$$

It is widely either assumed or understood that the statistical shadowing function $S_{\mathrm{S}}(\nu_1, \nu_2, h_0, \zeta_0)$ is statistically independent of the scattered field, leading to

$$\sigma_{\mathrm{S}} = \sigma_{\mathrm{S}}^{\mathrm{Un}} \times S_2, \tag{60}$$

where

$$\begin{aligned} \sigma_{\mathrm{S}}^{\mathrm{Un}} &= \int\int\int\int E_{\mathrm{S}}(\xi_0, \gamma_0) \times E_{\mathrm{S}}^{*}(\xi_0', \gamma_0') p(\xi_0, \gamma_0, \xi_0', \gamma_0') \, \mathrm{d}\xi_0 \, \mathrm{d}\gamma_0 \, \mathrm{d}\xi_0' \, \mathrm{d}\gamma_0' \\ S_2 &= \int\int\int\int p_{\mathrm{Sh}}(\nu_1, \nu_1, \xi_0, \gamma_0, \xi_0', \gamma_0') \, \mathrm{d}\xi_0 \, \mathrm{d}\gamma_0 \, \mathrm{d}\xi_0' \, \mathrm{d}\gamma_0'. \end{aligned} \tag{60a}$$

$\sigma_{\mathrm{S}}^{\mathrm{Un}}$ denotes the unshadowed scattering coefficient and S_2 the bistatic average shadowing function. As shown by Sancer [3], with the geometric optics approximation performed from the Kirchhoff approach, since the scattered field E_{S} becomes independent of the surface heights ξ_0 and slopes γ_0, (60) is verified. On the other hand, as proved by Bourlier *et al* [7, 8], with the Kirchhoff approach of first order (single scattering), (60) cannot be applied because the scattered field depends on $\{\xi_0, \gamma_0\}$.

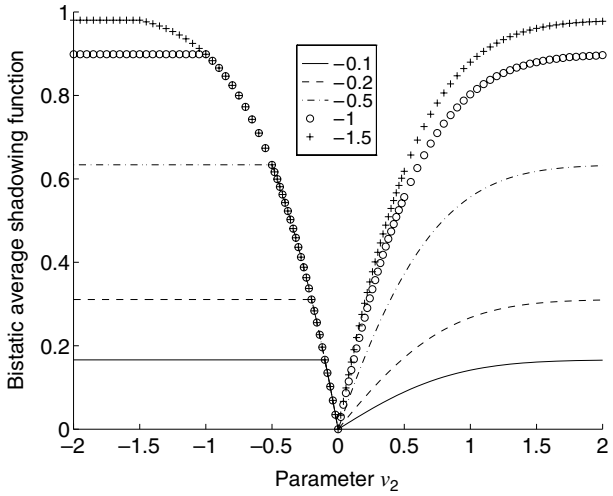

Figure 17. Average bistatic shadowing function versus ν_2 for a given ν_1 with an uncorrelated Gaussian process. The length observation is assumed to be infinite and the Smith formulation is used.

If the correlation between $\{\xi_0, \gamma_0, \xi_0', \gamma_0'\}$ is assumed to be negligible, then S_2 becomes from (17)

$$S_2 = \left[\int_{-\infty}^{\infty}\int_{-\infty}^{\infty} p_{\mathrm{Sh}}(\nu_1, \nu_2, \xi_0, \gamma_0)\,\mathrm{d}\xi_0\,\mathrm{d}\gamma_0\right]^2 = [S(\nu_1, \nu_2)]^2. \tag{61}$$

With the Smith approach (50) given for an uncorrelated Gaussian process and an infinite observation length, we obtain

$$S_{\mathrm{S}}(\nu_1, \nu_2) = \begin{cases} [\mathrm{erf}(\nu_1) + \mathrm{erf}(\nu_2)]/\{2[1 + \Lambda(\nu_1) + \Lambda_2(\nu_2)]\} & \text{if} \quad \nu_2 \geqslant 0 \\ [1 + \mathrm{erf}(\nu_2)]/\{2[1 + \Lambda(\nu_2)]\} & \text{if} \quad -\nu_1 \leqslant -\nu_2 < 0 \\ [1 + \mathrm{erf}(\nu_1)]/\{2[1 + \Lambda(\nu_1)]\} & \text{if} \quad -\infty \leqslant -\nu_2 < -\nu_1. \end{cases} \tag{62}$$

In figure 17 the bistatic average shadowing function is plotted versus the parameter ν_2 for a given ν_1. For a very rough surface (high standard deviation of slopes σ, i.e. $\nu_i = \mu_i/\sigma\sqrt{2}$ small), the shadowing function decreases quickly. For incidence near 90°, corresponding to $\nu_i \to 0$, the surface is highly shaded ($S_{\mathrm{S}} \to 0$). In contrast, for normal incidence ($|\nu_i|$ close to 2), the whole surface is illuminated ($S_{\mathrm{S}} = 1$). With respect to ν_2, the bistatic average shadowing function is not even since $S_{\mathrm{S}}(\nu_1, \nu_2) \neq S_{\mathrm{S}}(\nu_1)S_{\mathrm{S}}(\nu_2)$ for $\nu_2 \geqslant 0$.

The roughness of a random surface is characterized by the product $k\omega$ with ω the surface height rms, and k the wavenumber equal to $2\pi/\lambda$, where λ denotes the electromagnetic wavelength. The perturbation approach is valid when the surface height rms ω is small compared with the wavelength λ. The stationary phase method formulated from the Kirchhoff approach is valid when $k\omega \gg 1$, meaning $\omega \gg \lambda$. We have proved that the statistical shadowing function $S(\nu_1, \nu_2, \xi_0, \gamma_0, y_0)$ (see figure 13) modified the height distribution, meaning that ω_{Sh} with shadow depends on the incidence and scattering angles within $\{\nu_1, \nu_2\}$ for a bistatic configuration.

For example, from (50), ω_{Sh} becomes

$$\left(\frac{\omega_{\mathrm{Sh}}}{\omega}\right)^2 = \frac{2}{\sqrt{\pi}}\int_{-\infty}^{\infty} h_0^2 \exp(-h_0^2)\left[1 - \frac{1}{2}\mathrm{erfc}(h_0)\right]^L \mathrm{d}h_0, \tag{63}$$

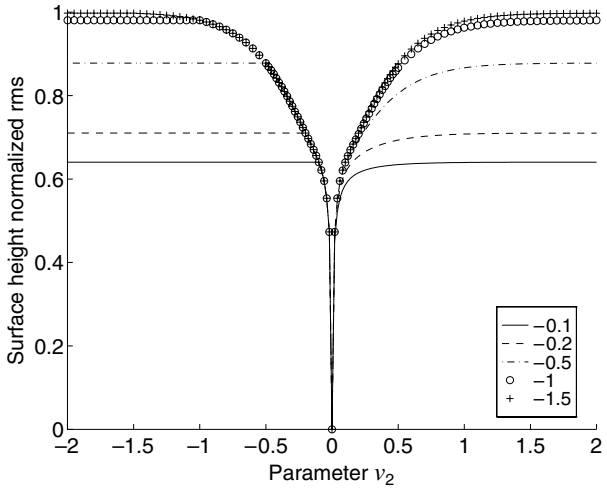

Figure 18. Surface-height-normalized rms $\omega_{\mathrm{Sh}}/\omega$ with shadow versus v_2 for a given v_1 with an uncorrelated Gaussian process. The length observation is assumed to be infinite and the Smith formulation is used.

with $L = \{\Lambda(v_1) + \Lambda(v_2), \Lambda(v_2), \Lambda(v_1)\}$ according to cases (a), (b) and (c). In figure 18, $\omega_{\mathrm{Sh}}/\omega$ is represented versus v_2 for a given v_1. We observe that the ratio $\omega_{\mathrm{Sh}}/\omega$ decreases when $\{|v_1|, |v_2|\}$ tend to zero, corresponding to either grazing incidence angles or larger surface slope rms, and the surface roughness becomes smaller.

5.3. Prospect

The effect of the observation length has only been investigated theoretically. Articles [9, 10] present, for an uncorrelated process, the effect of the observation length on the derivations of the emissivity and reflectivity with the shadowing function in the infrared band from a two-dimensional rough sea surface. The average shadowing function increases when the observation length decreases. As in the single-scattering problem, a scattering problem with multiple scattering which can be treated from the first- and second-order Kirchhoff approximations requires knowledge of the statistical shadowing function with multiple reflection. The prospect of this paper is to extend the statistical shadowing function with single reflection to that with multiple reflection. This aspect is presented in the second paper and simulations are made with respect to the observation length.

Since natural surfaces such as the sea are two dimensional, it will also be interesting to extend the formulation exposed in this paper to a two-dimensional rough surface. From the Smith formulation and for an infinite observation length, Bourlier *et al* [14] treated this problem on the average monostatic shadowing function for uncorrelated and correlated Gaussian processes.

Acknowledgments

The authors would like to thank the reviewers of the paper for their relevant comments.

Appendix. Conditional probability derivation of the Ricciardi–Sato approach

This appendix gives the derivation of the conditional probability obtained from the Ricciardi–Sato approach for any uncorrelated process.

Substituting (9) into (5*a*), we have for $n = 1$

$$I_1 = g_{\mathrm{W}} \times \mu\Lambda \int_0^l p(\xi_0 + \mu l_1)\,\mathrm{d}l_1 = \Lambda[P(\xi_0 + \mu l) - P(\xi_0)], \tag{A.1}$$

with P a primitive of p defined as

$$P = \int p(\xi)\,\mathrm{d}\xi. \tag{A.2}$$

For $n = 2$, we have from (9) and (5*a*)

$$I_2 = g_{\mathrm{W}} \times (\mu\Lambda)^2 \int_0^l p(\xi_0 + \mu l_1)\,\mathrm{d}l_1 \left[\int_{l_1}^l p(\xi_0 + \mu l_2)\,\mathrm{d}l_2\right]. \tag{A.3}$$

Using (A.2), the integration over l_2 yields

$$I_2 = g_{\mathrm{W}} \times \mu\Lambda^2 \int_0^l p(\xi_0 + \mu l_1)[P(\xi_0 + \mu l) - P(\xi_0 + \mu l_1)]\,\mathrm{d}l_1. \tag{A.4}$$

Writing that

$$\int p(\xi_0 + \mu l_1) P(\xi_0 + \mu l_1)\,\mathrm{d}l_1 = \frac{1}{2\mu}[P(\xi_0 + \mu l_1)]^2, \tag{A.5}$$

the integration over l_1 leads to

$$I_2 = g_{\mathrm{W}} \times \tfrac{1}{2}\{\Lambda[P(\xi_0 + \mu l) - P(\xi_0)]\}^2. \tag{A.6}$$

Substituting (9) into (5*a*), we have for $n = 3$

$$I_3 = g_{\mathrm{W}} \times (\mu\Lambda)^3 \int_0^l p(\xi_0 + \mu l_1)\,\mathrm{d}l_1 \left\{\int_{l_1}^l p(\xi_0 + \mu l_2)\,\mathrm{d}l_2 \left[\int_{l_2}^l p(\xi_0 + \mu l_3)\,\mathrm{d}l_3\right]\right\}. \tag{A.7}$$

Using the same method as previously, we show

$$I_3 = g_{\mathrm{W}} \times \tfrac{1}{6}\{\Lambda[P(\xi_0 + \mu l) - P(\xi_0)]\}^3. \tag{A.8}$$

Finally, we show by recurrence that for any $n \geqslant 1$, we obtain

$$I_n = g_{\mathrm{W}} \times \frac{1}{n!}\{\Lambda[P(\xi_0 + \mu l) - P(\xi_0)]\}^n. \tag{A.9}$$

Thus, we obtain from (3)

$$\begin{aligned} g_{\mathrm{R}}(\mu, F, l) &= g_{\mathrm{W}} \times \sum_{n=0}^{\infty} \frac{\{-\Lambda[P(\xi_0 + \mu l) - P(\xi_0)]\}^n}{n!} \\ &= g_{\mathrm{W}} \times \exp\{-\Lambda[P(\xi_0 + \mu l) - P(\xi_0)]\}. \end{aligned} \tag{A.10}$$

References

[1] Beckmann P and Spizzichino A 1963 *The Scattering of Electromagnetic Waves from Rough Surfaces* Part I *Theory* (London: Pergamon)

[2] Ulaby F T, Moore R K and Fung A K 1982 *Microwave Remote Sensing* vol 2 (Reading, MA: Addison-Wesley)

[3] Sancer M I 1969 Shadow-corrected electromagnetic scattering from a randomly rough surface *IEEE Trans. Antennas Propag.* **17** 577–85

[4] Wagner R J 1986 Shadowing of randomly rough surfaces *J. Opt. Soc. Am.* **41** 138–47

[5] Smith B G 1967 Lunar surface roughness, shadowing and thermal emission *J. Geophys. Res.* **72** 405–67

[6] Smith B G 1967 Geometrical shadowing of a random rough surface *IEEE Trans. Antennas Propag.* **15** 668–71
[7] Bourlier C, Berginc G and Saillard J 2001 Bistatic scattering coefficient from one- and two-dimensional random surfaces using the stationary phase and scalar approximation with shadowing effect—comparisons with experiments and application to the sea surface *Waves Random Media* **2** 91–118
[8] Bourlier C, Berginc G and Saillard J 2001 Theoretical study of the Kirchhoff integral from two-dimensional randomly rough surface with shadowing effect—application on the backscattering coefficient for a perfectly conducting surface *Waves Random Media* **2** 119–47
[9] Bourlier C, Saillard J and Berginc G 2000 Effect of the observation length on the two-dimensional shadowing function of the sea surface: application on infrared 3–13 μm emissivity *Appl. Opt.* **39** 3433–42
[10] Bourlier C, Saillard J and Berginc G 2000 Theoretical study on two-dimensional Gaussian rough sea surface emission and reflection in the infrared frequencies with shadowing effect *IEEE Trans. Geosci. Remote Sens.* **39** 379–92
[11] Ricciardi L M and Sato S 1986 On the evaluation of first passage time densities for Gaussian processes *Signal Process.* **11** 339–57
[12] Ricciardi L M and Sato S 1983 A note on first passage time problems for Gaussian processes and varying boundaries *IEEE Trans. Inf. Theory* **29** 454–7
[13] Brokelman R A and Hagfors T 1967 Note of the effect of shadowing on the backscattering of waves from a random rough surface *IEEE Trans. Antennas Propag.* **14** 621–7
[14] Bourlier C, Saillard J and Berginc G 2000 The shadowing function *PIER (Prog. Electromagn. Res., EMW)* ed J A Kong **27** 226–87
[15] Bourlier C, Saillard J and Berginc G 2000 Effect of correlation between shadowing and shadowed points on the Wagner and Smith monostatic one-dimensional shadowing functions *IEEE Trans. Antennas Propag.* **48** 437–46